

AD-A079 470

MASSACHUSETTS INST OF TECH CAMBRIDGE DEPT OF MATERIA--ETC F/6 20/3
MOLECULAR ORBITALS AND SUPERCONDUCTIVITY.(U)
DEC 79 K H JOHNSON, D D VVEDENSKY

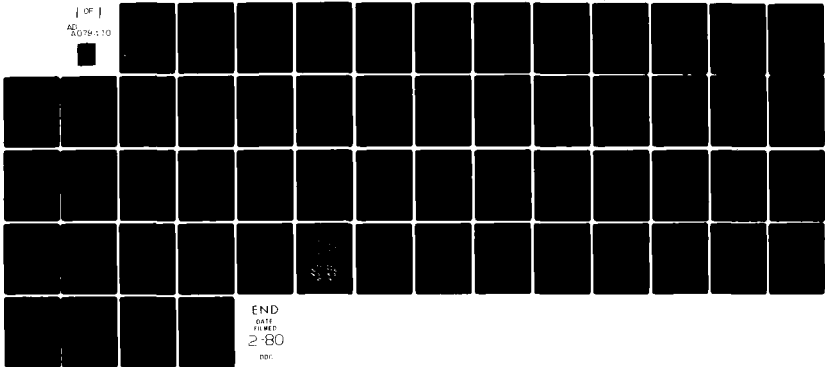
N00014-75-C-0970

UNCLASSIFIED

11

NL

[OF]
AD
5079:10



END
DATE
FILMED
2-80
DPR

UNCLASSIFIED

SECURITY CLASSIFICATION OF THIS PAGE (When Data Entered)

(12)

LEVEL

REPORT DOCUMENTATION PAGE

READ INSTRUCTIONS BEFORE COMPLETING FORM

1. REPORT NUMBER <u>14 11</u>	2. GOVT ACCESSION NO.	3. RECIPIENT'S CATALOG NUMBER
4. TITLE (and Subtitle) <u>MOLECULAR ORBITALS AND SUPERCONDUCTIVITY</u>		5. TYPE OF REPORT & PERIOD COVERED <u>9 Interim Report</u>
7. AUTHOR(s) <u>K. H. Johnson, D. D. Nvedensky, and R. P. Messmer</u>		6. PERFORMING ORG. REPORT NUMBER
8. PERFORMING ORGANIZATION NAME AND ADDRESS Department of Materials Science and Engineering Massachusetts Institute of Technology Cambridge, Massachusetts 02139		9. CONTRACT OR GRANT NUMBER(s) <u>15 N00014-75-C-0970</u>
11. CONTROLLING OFFICE NAME AND ADDRESS Office of Naval Research Department of the Navy Arlington, Virginia 22217		10. PROGRAM ELEMENT, PROJECT, TASK AREA & WORK UNIT NUMBERS Task No. NR056-596
14. MONITORING AGENCY NAME & ADDRESS (if different from Controlling Office) <u>16 59</u>		12. REPORT DATE <u>11 31 December 79</u>
		13. NUMBER OF PAGES
		15. SECURITY CLASS. (of this report) Unclassified
		18a. DECLASSIFICATION/DOWNGRADING SCHEDULE

16. DISTRIBUTION STATEMENT (of this Report)
Approval for public release; distribution unlimited.

17. DISTRIBUTION STATEMENT (of the abstract entered in Block 20, if different from Report)

DDC
RECEIVED
JAN 16 1980
A

18. SUPPLEMENTARY NOTES

19. KEY WORDS (Continue on reverse side if necessary and identify by block number)
molecular orbitals; superconductivity; magnetism
80 1 15 012

20. ABSTRACT (Continue on reverse side if necessary and identify by block number)
A real-space molecular-orbital description of electronic wavefunctions which are postulated to be the precursors of the superconducting state in metals, alloys, compounds, and noncrystalline materials is presented, based on self-consistent-field X-alpha scattered-wave (SCF-X_α-SW) molecular-orbital calculations for clusters representing the local molecular environments in these materials. It is shown through a variety of examples that there is a persistent correlation between the occurrence of superconductivity in a

ADA 079470

DDC FILE COPY

409463

[Handwritten signature]

UNCLASSIFIED

SECURITY CLASSIFICATION OF THIS PAGE (When Data Entered)

material and the existence of molecular orbitals at the Fermi energy with coherent (i.e., in-phase) spatially extended (e.g., $p\pi$, d_6 , d_{z^2} , or sc) bonding atomic-orbital components. It is also argued that, while these individual molecular-orbital components are usually "one-dimensional" or "two-dimensional" in nature, the composite precursor superconducting state of a material arises from a coherent three-dimensional "network" or "array" of these components. It is further demonstrated through examples that for each such orbital component, covalent bond overlap in a line or plane of atoms is enhanced by the interaction of atoms not in that line or plane, as shown by the $p\pi$ - po^* bonding-antibonding interaction in aluminum and by metal-ligand interactions in A15 and layered transition-metal compounds. This description of the precursor superconducting state is consistent with the original conjectures of London and Slater that the superconducting-state wavefunction is "molecular" in nature, "rigid" in character, and of wide spatial extent, from which observed physical properties (e.g., diamagnetism and nondissipative electrical currents) of the superconducting state logically follow. This molecular-orbital description is further argued to be consistent with Cooper's concept of electron pairing in the superconducting state through a net attractive electron-electron interaction but differs from the usual viewpoint in attributing this attractive interaction directly to real-space chemical-bond-like formation rather than to electron-phonon coupling *per se*. The two points of view, however, are not necessarily incompatible. The above molecular-orbital criteria for superconductivity are diametrical to those for the occurrence of local magnetic moments and ferro- and antiferromagnetism, namely the existence of spin-polarized spatially localized antibonding (e.g., do^* and $d\pi^*$) molecular orbitals near the Fermi energy. These criteria therefore provide a simple conceptual basis for understanding the generally mutually exclusive incidence of superconductivity and magnetism among the elements of the periodic table, although they can also be used to explain the occasional coexistence of superconductivity and ferromagnetism or antiferromagnetism in some materials. The molecular-orbital criteria for superconductivity complement existing formal theories in that they appear to explain simply and directly certain observed chemical trends of superconductivity, such as those frequently emphasized by Matthias, and are naturally applicable to superconducting materials lacking long-range crystalline order, such as solid-solution alloys, amorphous alloys, and small particles. Finally, it appears that the molecular-orbital approach can be used to explain from simple considerations why some materials (e.g., Cu, Ag, and Au) are neither superconducting nor magnetic, to rule out certain types of substances (e.g., certain classes of quasi-one-dimensional organic solids; metallic hydrogen at attainable high pressures) as possible superconductors, and to suggest ways of systematically improving existing classes or synthesizing new classes of superconducting materials.

UNCLASSIFIED

SECURITY CLASSIFICATION OF THIS PAGE (When Data Entered)

ABSTRACT

A real-space molecular-orbital description of electronic wavefunctions which are postulated to be the precursors of the superconducting state in metals, alloys, compounds, and noncrystalline materials is presented, based on self-consistent-field X-alpha scattered-wave (SCF-X α -SW) molecular-orbital calculations for clusters representing the local molecular environments in these materials. It is shown through a variety of examples that there is a persistent correlation between the occurrence of superconductivity in a material and the existence of molecular orbitals at the Fermi energy with coherent (i.e., in-phase) spatially extended (e.g., $p\pi$, $d\delta$, d_{22} , or $s\sigma$) bonding atomic-orbital components. It is also argued that, while these individual molecular-orbital components are usually "one-dimensional" or "two-dimensional" in nature, the composite precursor superconducting state of a material arises from a coherent three-dimensional "network" or "array" of these components. It is further demonstrated through examples that for each such orbital component, covalent bond overlap in a line or plane of atoms is enhanced by the interaction of atoms not in that line or plane, as shown by the $p\pi$ - $p\sigma^*$ bonding-antibonding interaction in aluminum and by metal-ligand interactions in A15 and layered transition-metal compounds. This description of the precursor superconducting state is consistent with the original conjectures of London and Slater that the superconducting-state wavefunction is "molecular" in nature, "rigid" in character, and of wide spatial extent, from which observed physical properties (e.g., diamagnetism and nondissipative electrical currents) of the superconducting state logically follow. This molecular-orbital description is further argued to be consistent with Cooper's concept of electron pairing in the superconducting state through a net attractive electron-electron interaction but differs from the usual

viewpoint in attributing this attractive interaction directly to real-space chemical-bond-like formation rather than to electron-phonon coupling per se. The two points of view, however, are not necessarily incompatible. The above molecular-orbital criteria for superconductivity are diametrical to those for the occurrence of local magnetic moments and ferro- and antiferromagnetism, namely the existence of spin-polarized spatially localized antibonding (e.g., $d\sigma^*$ and $d\pi^*$) molecular orbitals near the Fermi energy. These criteria therefore provide a simple conceptual basis for understanding the generally mutually exclusive incidence of superconductivity and magnetism among the elements of the periodic table, although they can also be used to explain the occasional coexistence of superconductivity and ferromagnetism or antiferromagnetism in some materials. The molecular-orbital criteria for superconductivity complement existing formal theories in that they appear to explain simply and directly certain observed chemical trends of superconductivity, such as those frequently emphasized by Matthias, and are naturally applicable to superconducting materials lacking long-range crystalline order, such as solid-solution alloys, amorphous alloys, and small particles. Finally, it appears that the molecular-orbital approach can be used to explain from simple considerations why some materials (e.g., Cu, Ag, and Au) are neither superconducting nor magnetic, to rule out certain types of substances (e.g., certain classes of quasi-one-dimensional organic solids; metallic hydrogen at attainable high pressures) as possible superconductors, and to suggest ways of systematically improving existing classes or synthesizing new classes of superconducting materials.

I. INTRODUCTION

The Bardeen-Cooper-Schrieffer (BCS) theory of superconductivity¹ ascribes the onset of the superconducting state of a crystal at the transition temperature, T_c , to electrons attractively paired via thermal vibrations of the lattice (phonons). The BCS formula for T_c is

$$T_c \sim \theta_D \exp [-1/VN(\epsilon_F)], \quad (1)$$

where θ_D is the Debye temperature, V is the net attractive potential between electrons in Cooper pairs² induced by the electron-phonon interaction, and $N(\epsilon_F)$ is the electronic density of states at the Fermi energy. The BCS theory together with its strong-coupling extension has been eminently successful in accounting for the physical properties, e.g., nondissipative current, diamagnetism, and thermodynamics of the superconducting state, and has correlated many experimental data in terms of a few basic parameters. Nevertheless, it has often been emphasized by Matthias³ that the BCS theory and formal extensions thereof do not satisfactorily explain the observed dependence of superconductivity on crystal structure and chemistry (especially for transition metals, alloys, and compounds), do not address the mutually exclusive incidence of superconductivity and magnetism for the elements in the periodic table, and are not very useful for predicting new superconducting materials. The existence of superconducting materials possessing only short-range structural order, such as superconducting amorphous alloys⁴ and superconducting metal particles down to $\sim 50 \text{ \AA}$ in size,^{5,6} also, strictly speaking, lies outside the domain of BCS theory. The BCS theory, in its conventional form, is based on the traditional concepts of long-range crystalline order and momentum (\vec{k}) space, leading to coherence lengths of the superconducting state that greatly exceed the short-range order and electron mean free path characteristic of amorphous

and small-particle superconductors. This suggests the need for a local chemical-bonding or "real-space" molecular description of the superconducting state. Indeed, London^{7,8} in his phenomenological approach to superconductivity discusses the possibility of developing a molecular description of the superconducting state (see Chapter E of Ref. 8), and Slater⁹ in his classic papers on the subject provides a qualitative description of the spatial character of the superconducting-state wavefunction. With speculations that mechanisms other than electron-phonon coupling can attractively pair electrons in the superconducting state,^{3,10,11} a molecular criterion that accounts for the known chemical trends in the occurrence of superconductivity would be a useful tool in the continuing effort to identify new classes of superconducting materials.

The systematic trends of T_c with valence-electron-per-atom ratio³ and the difficulty of calculating BCS parameters for transition metals, their alloys, and compounds have prompted the development of rudimentary chemical models,¹²⁻¹⁴ based on atomic d orbitals and aimed primarily at the estimation of T_c . However, these models are not easily generalized to non-transition-metal superconductors and do not yield a real-space molecular description of the superconducting state. The most general chemical approach to superconductivity is that of Krebs,¹⁵ who has suggested that superconductivity is possible only if the normal chemical bonding system in the crystal or parts of the crystal permits the construction of a molecular wavefunction which for at least one space direction is not intersected by plane or conical nodal surfaces, and if the corresponding electron band is not fully occupied. Note that Krebs attempts only to account for the incidence of superconductivity through qualitative chemical bonding arguments and not the evaluation of a specific electron-pairing mechanism and T_c .

In this paper, we present a real-space molecular-orbital description

and criteria for the occurrence of the superconducting state in metals, alloys, compounds, and noncrystalline materials, including amorphous solids and small particles. This theoretical approach to superconductivity makes direct use of the results of first-principles self-consistent-field X-alpha scattered-wave (SCF-X α -SW) molecular-orbital calculations for clusters representing the local molecular environments in these materials. The SCF-X α -SW method¹⁶ is based on the combined use of the X α density-functional approximation¹⁷ to electron-electron exchange and correlation and the multiple-scattered-wave technique¹⁸ of solving the Schrödinger self-consistent-field molecular-orbital equations. In conjunction with the "transition-state" procedure^{16,17} for calculating electronic transitions between orbitals, this method leads to a description of both the ground and excited electronic states of a system. The calculation of different molecular orbitals for different spins allows one to consider the effects of magnetic spin polarization. Along with applications to a wide variety of polyatomic molecules,^{19,20} including biological macromolecules²¹⁻²³ and polymers,²⁴ this approach has been used successfully to elucidate the local bulk and surface electronic structures and properties of solids,²⁵⁻²⁷ e.g., crystalline semiconductors and localized defects and impurities therein,²⁸⁻³¹ amorphous semiconductors,³² crystalline and amorphous metals and alloys³³⁻³⁸ including magnetic properties,^{35,37} molecular crystals,²⁴ and chemisorption on metal surfaces^{39,40} including the calculation of photoelectron emission intensities,^{41,42} electron-scattering cross sections,⁴³ and "shake-up" spectra⁴⁴ for chemisorbed species. These theoretical studies collectively suggest that short-range order and local chemical bonding largely determine the measurable electronic structures and properties of many types of materials, whether ordered or disordered.

In view of the complementary natures of superconductivity and magnetism, it should be noted that spin-unrestricted SCF-X α -SW cluster molecular-orbital

studies³⁵ indicate that the local magnetic moments of Fe and Mn impurities in crystalline copper above the Kondo temperature are associated with the existence of spin-polarized antibonding (σ^* and π^*) Fe(d)-Cu(s,d) molecular orbitals near the Fermi energy (see Figs. 10, 12, and 13 of Ref. 35). Similar cluster models for ferromagnetic bcc crystalline α -iron^{37,26} suggest that the onset of collective magnetism below the Curie temperature and the persistence of "spin clusters" above the Curie temperature are associated with the existence of spin-polarized antibonding (σ^* and π^*) Fe(d)-Fe(d) molecular orbitals near the Fermi energy of the type shown in Fig. 1. Recent spin-polarized SCF- $X\alpha$ -SW cluster models for amorphous iron-boron and iron-phosphorus alloys³⁸ are also in good quantitative agreement with measured magnetic properties and clearly show the key role of antibonding molecular orbitals at the Fermi energy in determining how alloying alters the magnetic properties of iron. For the sake of completeness, it may also be noted that the SCF- $X\alpha$ -SW method has been applied to iron-containing biological molecules such as ferredoxin²² and hemoglobin²³ and the results used to explain observed magnetic properties (including the calculation of magnetic hyperfine parameters²³) as functions of temperature and oxygenation, respectively. Finally, the spin-unrestricted SCF- $X\alpha$ -SW method, in conjunction with the transition-state procedure,^{16,17} has recently been employed with good results to calculate, from first principles, ferromagnetic and antiferromagnetic exchange coupling constants (Heisenberg exchange integrals) for transition-metal cluster coordination complexes.⁴⁵ The most general finding of the theoretical studies of magnetic substances summarized above is that both local and collective forms of magnetism are associated with the occurrence of antibonding spin-polarized molecular orbitals (e.g., the $d\sigma^*$ and $d\pi^*$ components in Fig. 1) near the Fermi energy.

Because of the complementary natures of magnetism and superconductivity,

it is reasonable to expect that SCF- $X\alpha$ -SW cluster molecular-orbital studies of superconducting materials can also provide insight into the role of chemical bonding in determining the superconducting state. Indeed, it will be shown in this paper that the molecular-orbital criteria for the occurrence of superconductivity and magnetism are diametrical, thereby offering a simple explanation for the mutually exclusive occurrence of these phenomena in a material at the same temperature and pressure. The orbital criteria for superconductivity will further be shown to be consistent with Cooper's² concept of electron pairing through a net attractive electron-electron interaction (V in Eq. 1) but differs from BCS theory¹ in attributing this attractive interaction directly to real-space chemical-bond formation at the Fermi energy, rather than to electron-phonon coupling per se. Finally the molecular-orbital approach presented herein will be used to explain why some metals (e.g., Cu, Ag, and Au) are neither superconducting nor magnetic and to provide a reliable theoretical tool for predicting new superconducting materials.

II. CLUSTER MOLECULAR ORBITALS AND BAND STRUCTURE

The relationships of SCF- $X\alpha$ -SW cluster molecular-orbital energy levels and densities of states to the corresponding crystal band structures and densities of states calculated from Bloch's theorem and measured spectroscopically have been discussed in previous publications and reports for the examples of copper,^{33,35} nickel,³⁷ aluminum,^{34,39} and iron.³⁷ Nevertheless, in order to clarify the use of cluster molecular orbitals as a basis for superconductivity, we point out some specific similarities and differences between cluster electronic structure and crystal band structure.

For simplicity, consider first the example of an isolated benzene molecule, the π orbitals of which are shown schematically on the left side

of Fig. 2. The π_1 orbital, which is occupied by two spin-paired electrons and has the energy level ϵ_1 , is the most strongly bonding of the $p\pi$ molecular orbitals, whereas the degenerate π_2 and π_3 orbitals, which together are occupied by four spin-paired electrons and have the energy level $\epsilon_{2,3}$, are relatively weakly bonding. The unoccupied π_3^* orbital is strongly antibonding, while the unoccupied π_1^* and π_2^* orbitals are weakly antibonding. Because of the one-dimensional periodicity of the carbon atoms around the benzene ring, the molecular orbitals can be expressed in symmetrized Bloch form,⁴⁶ resulting in the discrete one-dimensional "k-space" band profile shown schematically on the right side of Fig. 2. The "Fermi energy" ϵ_F separates the occupied states from the unoccupied ones. In this particular example, there is a simple one-to-one correspondence between the "real-space" molecular orbitals and "k-space" band structure, as indicated by the connecting lines in Fig. 2. It has often been noted that the diamagnetic "ring currents" induced in benzene and other aromatic molecules through the response of the $p\pi$ electrons to an external magnetic field are nondissipative currents similar in some (but not all) respects to the persistent currents of a superconducting ring.^{8,47,48}

On the other hand, the molecular orbitals of a finite cluster representing the local molecular environment in a crystal transform according to the irreducible representations of the cluster point symmetry group and therefore are not generally equivalent on a one-to-one basis to Bloch band eigenstates of the crystal, except at the points in \vec{k} -space which have the full cluster point group symmetry. For example, the $\Gamma(\vec{k}=0)$ Bloch state has the full O_h point-group symmetry in a cubic crystal. Nevertheless, it is possible to construct combinations of degenerate Bloch states of different

\vec{k} (the so-called "star" of the wavevector) that transform according to the irreducible representations of the cluster point group.⁴⁹ From this, one can conclude that there should be a reasonably close correspondence between cluster and crystal densities of states. Examples of such correspondence will be found in Refs. 33, 34, 37, and 39.

As an illustrative application of the above concepts to a superconducting metal, consider the example of aluminum. In Fig. 3, the SCF-X α -SW molecular-orbital energy levels of a 19-atom cluster representing the local environment of fcc crystalline aluminum up to second-nearest neighbors³⁴ are compared with the energy bands of the crystal shown along principal symmetry directions of the Brillouin zone. The Al₁₉ cluster density of states, based on a Gaussian broadening of the discrete molecular-orbital energy levels of the type described in Refs. 33 and 34, is shown in Fig. 4. A detailed comparison of cluster and crystal densities of states for aluminum, including a cluster molecular-orbital analysis of the density of states derived from photoemission spectra, is presented in Ref. 34.

Like the results described in Ref. 35 for a 19-atom cluster representing crystalline copper, there is a remarkably close correspondence of the total energy span of the Al₁₉ cluster orbitals to the band width of the crystal and a close relationship between individual cluster orbitals to particular energy-band Bloch eigenstates or combinations thereof. For example, the lowest occupied cluster energy level, $1a_{1g}$, shown in Fig. 3 is the discrete molecular-orbital analogue of the $\Gamma_1(\vec{k}=0)$ s-band Bloch state. Among the highest occupied and lowest unoccupied cluster orbitals, the fully occupied t_{1g} level corresponds mainly to Σ_3 p-band states just below the Fermi energy ϵ_F , the partially occupied $4t_{1u}(\epsilon_F)$ level corresponds to combinations of degenerate Σ_3 , Σ_1 , and Δ_1 p-band states at the Fermi energy, and the empty t_{2g} level corresponds

primarily to Σ_1 p-band states just above the Fermi energy. The t_{1g} , $4t_{1u}(\epsilon_F)$, and $2t_{2g}$ molecular orbitals are responsible for the peak in the cluster density of states at the Fermi energy evident in Fig. 4 and are the discrete analogues of the parallel Σ_3 and Σ_1 p bands largely responsible for the peak in the crystalline band-structure and photoemission densities of states around the Fermi energy.³⁴

As will be shown in the following section of the paper, the $t_{1u}(\epsilon_F)$ cluster molecular orbital is key to understanding the real-space nature of the superconducting state of aluminum. The wavefunction contour maps of this orbital, plotted in the (200) and (110) crystallographic planes, are shown in Figs. 5 and 6, respectively. The solid and dashed contours represent positive and negative regions, respectively, of the molecular-orbital wavefunction. Regions of net overlap between contours of the same sign are bonding, whereas regions of positive and negative contours separated by nodes are antibonding. The most striking feature of Figs. 5 and 6 is the "one-dimensional" π -bonding character of the Al p orbitals along the "horizontal" direction of each figure, much like the one-dimensional p orbitals of the benzene molecule shown in Fig. 2. However, in contrast to benzene, where the $p\pi_1$ molecular orbital lies well below the Fermi energy, the $p\pi$ -bonding orbital of aluminum is located exactly at the Fermi energy at $T = 0^\circ\text{K}$. Unlike benzene, moreover, there is also a "one-dimensional" σ^* -antibonding component between the Al p orbitals along the "vertical" direction in Figs. 5 and 6, which, through electron-electron repulsion, isolates the $p\pi$ orbitals along parallel lines of atoms and synergistically promotes covalent $p\pi$ bond overlap within each line of atoms. Although Figs. 5 and 6 imply anisotropy in each $t_{1u}(\epsilon_F)$ molecular-orbital component, the triple degeneracy of this orbital leads to equivalent $p\pi$ -bonding and $p\sigma^*$ -antibonding components along the two complementary orthogonal crystal directions and therefore to an isotropic three-dimensional orbital charge distribution. As cluster size

is systematically increased to include more shells of atoms in the crystal (e.g., see the 43-atom results in Ref. 34), each $p\pi$ -bonding and $p\sigma^*$ -antibonding orbital component at the Fermi energy expands spatially and, in the limit of a large number of atoms, forms a coherent macroscopic molecular orbital of the type shown in Fig. 7. A perspective drawing of $p\pi$ bonding along a line of atoms is shown in Fig. 8. This "real-space" character of aluminum molecular orbitals at the Fermi energy cannot be extracted easily from the conventional " \vec{k} -space" Bloch description of the crystal band structure, except in hindsight as an appropriate combination of Σ_1 , Σ_3 , and Δ_1 Bloch eigenstates, and thus has eluded solid-state physics.

III. CLUSTER MOLECULAR ORBITALS AND THE SUPERCONDUCTING STATE

The traditional view of the BCS and earlier theories of superconductivity^{1,8,9} is that the superconducting state of a crystal is a "special," highly ordered electronic state of large but finite coherence length, constructed from linear combinations of degenerate Bloch states of opposite momenta or wavevectors (\vec{k} , $-\vec{k}$) at the Fermi energy and occupied by spin-paired electrons between which there is a net attraction. In this section of the paper, we will attempt to establish that the above view is consistent with the real-space representation of the superconducting state as arising from discrete molecular orbitals at the Fermi energy with coherent, spatially extended bonding components, for which certain cluster molecular orbitals of the type described in the preceding section (the $p\pi$ - $p\sigma^*$ orbitals of aluminum) are precursors. One attractive feature of this concept is that it leads immediately to a simple explanation of the aforementioned similarity between the nondissipative diamagnetic ring currents associated with the $p\pi$ electrons of benzene (see Fig. 2) and other aromatic molecules^{8,47,48} and the persistent diamagnetic currents in a superconductor. Moreover, since the cluster molecular-orbital model is not dependent on the assumption of long-range crystalline order, it is applicable to amorphous⁴ and small-particle^{5,6} superconductors,

where \vec{k} is not a good quantum number, strictly speaking.

In the above picture, the attractive interaction responsible for electron pairing in the superconducting state occurs through the exclusive occupancy at the Fermi energy (for $T \sim 0^\circ\text{K}$) of spatially extended covalent bonding molecular-orbital components of the $p\pi$ type for p-electron materials like aluminum or, as will be shown below, bonding orbitals of the $d\delta$ and d_{z^2} type for transition metals and their compounds. This is not to imply that the phonons do not play a role in superconductivity, since the phonon spectrum and the concomitant electron-phonon interaction are byproducts of the attractive potential energy of the atoms associated with the chemical bond. The electron pairs are spatially delocalized over the "coherence length" of the appropriate bonding molecular orbital, e.g., the $p\pi$ components in Figs. 5, 6, and 7, in much the same fashion as the electron pairs are delocalized over the benzene $p\pi_1$ -electron ring in Fig. 2. Moreover, the electron-electron repulsion associated with the $p\sigma^*$ -antibonding components of Figs. 5 through 7 synergistically promotes the covalent pairing of electrons associated with the $p\pi$ -bonding components. Note that in the original paper by Cooper² on the concept of electron pairing in superconductivity and in the much earlier papers by Slater⁹ on the nature of the superconducting state, the attractive interaction responsible for the pairing of electrons of opposite Bloch wavevectors (\vec{k} , $-\vec{k}$) at the Fermi energy can, in retrospect, be identified directly with chemical bonding, without altering the basic ideas and respective formalisms in these papers.

Slater⁹ has also shown that if the superconducting state is characterized by a discrete energy level with a reasonably uniform wavefunction which is spatially delocalized over ~ 137 atomic diameters and then decays exponentially in a molecular fashion, this state acts like a huge "atom" or "molecule" and exhibits, for moderate applied magnetic fields, a large diamagnetism of the

type observed in superconductors and predicted by London's^{7,8} phenomenological theory of superconductivity. The cluster $p\pi$ - $p\sigma^*$ molecular-orbital wavefunction of aluminum described above is very much like the wavefunction described by Slater,⁹ especially as the cluster size is expanded to encompass many atoms (see Fig. 7). The "wide extension in space" of the superconducting-state wavefunction is also discussed by London (see p. 150 of Ref. 8). The electron pairs occupying this molecular orbital should not be viewed as propagating free electrons in the sense of ordinary conducting electrons, but rather as rigidly confined to the coherence length of the wavefunction (a hundred or more atoms, but not the entire crystal), like electrons confined as "standing deBroglie waves" in a large box of constant potential energy. The wide spatial extent of the superconducting-state molecular orbitals suggests from the uncertainty principle that the electron pairs occupying this orbital exist in the same center-of-mass momentum state. As discussed by London⁸ and Slater,⁹ such a wavefunction is unchanged by the application of an external magnetic field of moderate size. In other words, the electrons in this state, which represent a small fraction of the total number of electrons in the system, are prevented from "coiling up" like free electrons when the system is brought into a magnetic field, but stay essentially as they are without the magnetic field, as if "frozen."⁸ The synergistic $p\pi$ -bonding and $p\sigma^*$ -antibonding components of the molecular-orbital wavefunction shown in Fig. 7 are responsible for the "rigid" nature of the superconducting state of aluminum.

It is appropriate here to point out an interesting analogy between the present real-space concept of superconductivity and the coherent transmission of light by optical fibers. The spatially extended $p\pi$ -bonding molecular-orbital components of aluminum shown in Fig. 7 (and, as will be shown below, the $d\sigma$ -bonding orbitals of transition metals) can be viewed

simplistically as providing, through covalent bond overlap, quasi-one-dimensional "waveguides" for the standing deBroglie waves associated with the coherent superconducting-state electrons, in analogy to the way optical fibers act as electromagnetic waveguides for the coherent transmission of light. Indeed, the orthogonal $p\sigma^*$ -antibonding molecular-orbital components in Fig. 7 promote the covalent π overlap between Al p orbitals in each "waveguide channel," thereby isolating each "channel" from the others much like the independent optical fibers in a fiber bundle.

The nature of the supercurrent associated with such a wavefunction likewise follows from the original work of London⁸ and Slater.⁹ Classically, the electric current density produced by n electrons per unit volume of charge $-e$ moving with velocity \vec{v} is given by the formula

$$\vec{j} = -ne\vec{v}. \quad (2)$$

In an applied magnetic field of vector potential \vec{A} , the electron velocity is related to the electron momentum \vec{p} by the expression

$$m\vec{v} = \vec{p} - e\vec{A}/c. \quad (3)$$

Combining equations (2) and (3) and reformulating the resulting expression in quantum-mechanical terms, the electric current density associated with a state represented by a molecular-orbital wavefunction ψ occupied by n electrons is⁸

$$\vec{j} = (-ne\hbar/2m)(\psi^*\vec{\nabla}\psi - \psi\vec{\nabla}\psi^*) - (ne^2/mc)\vec{A}\psi^*\psi. \quad (4)$$

For example, one may substitute for ψ in the above expression a simple linear-combination-of-atomic-orbitals (LCAO) representation of the extended real-space superconducting-state molecular-orbital wavefunction, ψ_s , of aluminum shown in Fig. 7. Then the terms with the gradients, which correspond to the average value of ordinary electron-momentum carrying current, cancel each other because of symmetry, leaving for the net current density the purely diamagnetic term

$$\vec{j}_s = -ne^2\vec{A}|\psi_s|^2/mc. \quad (5)$$

Since n is the number of electrons in the superconducting-state molecular orbitals of probability density $|\psi_s|^2$, the product

$$n_s = n|\psi_s|^2 \quad (6)$$

represents the number of electrons per unit volume which are responsible for the current density (5). Note that in the cluster molecular-orbital representation of a superconductor, ψ_s corresponds to only one discrete energy level at the Fermi energy [the $4t_{1u}(\epsilon_F)$ level of the Al_{19} cluster in Fig. 3], so that n_s is only a small fraction of the total number of electrons of the system (the electrons in all the occupied cluster molecular orbitals of Fig. 3). Indeed, London⁸ has shown that, for a simply connected isolated superconductor and for given macroscopic boundary conditions, a single electronic state of wide spatial extent (such as the molecular orbital in Fig. 7) is sufficient to represent all currents realizable according to macroscopic electrodynamics. Substitution of Eq. (6) into Eq. (5) yields

$$\vec{j}_s = -n_s e^2 \vec{A} / mc, \quad (7)$$

Taking the curl of both sides of Eq. (7) yields the magnetic field expression

$$\vec{B} = \vec{\nabla} \times \vec{A} = -(mc/n_s e^2) \vec{\nabla} \times \vec{j}_s, \quad (8)$$

which is known as London's equation. London⁸ has shown from Eqs. (7) and (8) that the current \vec{j}_s produced by the magnetic field in a material of macroscopic size is confined to a thin surface layer and is parallel to the surface, it acts to shield the inner superconductor from the external magnetic field (the Meissner effect), and it is not subject to dissipation or electrical resistance through interaction with the lattice. Thus the "supercurrent" \vec{j}_s is of a fundamentally different character from ordinary electrical conduction.

For known superconductors, where $T_c < 25^\circ K$, the superconducting-state molecular orbitals ψ_s are exclusively occupied at the Fermi energy only for $T \sim 0^\circ K$. As T approaches T_c , thermally induced electronic excitations

gradually begin to depopulate these orbitals and to occupy otherwise empty orbitals lying close in energy to ψ_s . Most of the available orbitals above the Fermi energy are antibonding or nonbonding in the local chemical sense, as illustrated in Fig. 2 by the π_3^* and π_1^* , π_2^* orbitals, respectively, of the benzene molecule. They lack the coherent spatially extended bonding character of the superconducting-state orbitals ψ_s and therefore can be viewed as constituting the nonsuperconducting phase observed for $T > T_c$. Since the entropy of a phase depends essentially on the number of stationary states belonging to the phase, then the entropy of the superconducting phase, which is determined by a few orbitals ψ_s , is negligible compared with the entropy of the nonsuperconducting phase, which is determined by the manifold of excited-state orbitals. The effectively zero entropy of the superconducting phase is consistent with the high degree of order of the superconducting state. Slater⁹ has argued that the gradual onset of electronic transitions between the superconducting state and low-lying excited states, when translated into the language of thermodynamics, corresponds to the onset of the second-order transition between the superconducting and nonsuperconducting phases.

Since the SCF-X α -SW method satisfies Fermi statistics, the above-described excitations can be represented qualitatively by the cluster molecular-orbital model in conjunction with the transition-state concept.^{16,17} For example, the first allowed electronic transition in an Al₁₉ cluster representing superconducting aluminum (see Fig. 3) is between the $p\pi$ - $p\sigma^*$ molecular orbital $4t_{1u}(\epsilon_F)$ shown in Figs. 5 and 6 and the virtual $d p\sigma$ molecular orbital $2t_{2g}$. The $2t_{2g}$ molecular orbital lacks the coherent spatially extended character of the $4t_{1u}(\epsilon_F)$ orbital and is unoccupied in the ground state of the Al₁₉ cluster because there are no occupied d orbitals in the ground state of an Al atom. However, this molecular orbital becomes occupied even in the ground state when a transition-metal impurity such as Mn is substituted for

the central atom in an Al_{19} cluster, resulting in σ -type chemical bonding between the d orbitals of Mn and p orbitals of nearest-neighbor Al atoms, as indicated in the $t_{2g}(\epsilon_F)$ wavefunction contour map of Fig. 9. It will be shown below that such bonding is responsible for the degrading effect of transition-metal impurities on the superconducting state of aluminum. For pure Al_{19} , the transition-state energy of the $4t_{1u}(\epsilon_F) \rightarrow 2t_{2g}$ molecular-orbital excitation (see Fig. 3), which is the discrete cluster analogue of the onset of the phase transition between the superconducting and nonsuperconducting states of aluminum particles and crystals, is ~ 0.05 eV, implying a T_c well above room temperature for this small cluster. Of course, it is no more practical to think in terms of $p\pi$ -electron superconductivity in a 19-atom aluminum cluster than it is in an isolated benzene molecule, since no reasonably sized coherence length is attained. Nevertheless, as the cluster size is systematically increased by including successive shells of atoms in the crystal (e.g., in the 43-atom results described in Ref. 34), the energy gap between the $t_{1u}(\epsilon_F)$ $p\pi$ - $p\sigma^*$ molecular orbital at the Fermi energy and first unoccupied orbital decreases while the number of unoccupied orbitals immediately above the Fermi energy increases, implying a decreasing T_c with increasing cluster size. Superconductivity has, in fact, been observed for aluminum particles down to 50 \AA in diameter,^{5,6} which is roughly an order of magnitude less than Slater's⁹ estimate of the coherence length (137 atomic diameters = 388 \AA) and many orders of magnitude less than the coherence length for crystalline aluminum ($16,000 \text{ \AA}$)⁵⁰ derived from BCS theory. If one extrapolates the decreasing value of the molecular-orbital energy gap at the Fermi level with increasing cluster size to a 50 \AA particle, using a scaling procedure for the cluster energy levels analogous to that described by Slater,⁹ a gap of $\sim 10^{-4}$ eV is obtained, which implies a T_c of $\sim 1^\circ\text{K}$.

The measured value of T_c for small superconducting aluminum particles is 1.5 to 2.5°K,⁶ while T_c for bulk crystalline aluminum is 1.14°K.⁵⁰ As for the BCS formula (1) for T_c expressed in terms of the electronic density of states at the Fermi energy, $N(\epsilon_F)$, it should be emphasized that only the $p\pi$ -bonding molecular-orbital contribution to $N(\epsilon_F)$ (see Section II and Fig. 4) is pertinent to the superconducting property of aluminum.

In the above-described chemical picture, the well known mutually exclusive incidence of superconductivity and magnetism at a particular temperature (or pressure) in a material³ can be understood directly and simply from the exactly opposite molecular-orbital criteria for the occurrence of these two phenomena. For superconductivity, there must be a spin-paired molecular orbital at the Fermi energy with coherent spatially extended bonding components, e.g., the $p\pi$ components of aluminum described above and the ds components of transition metals to be discussed below. In contrast, for magnetism there must be a spin-polarized spatially localized exclusively antibonding molecular orbital at the Fermi energy, e.g., the $d\sigma^*-d\pi^*$ orbitals of ferromagnetic iron discussed in Section I (see Fig. 1) and the $d\sigma^*-d\pi^*$ orbitals of locally magnetic Fe and Mn impurities in a crystalline copper host above the Kondo temperature discussed in Ref. 35.

The above theoretical model for superconducting aluminum is also consistent with the observation that certain types of magnetic impurities in aluminum destroy its superconductivity, or at least lower T_c . A good example is Mn, whose effects in aluminum can be modeled in a fashion analogous to the treatment of Mn in copper (see Ref. 35) by substituting a Mn atom for the central Al atom in the 19-atom cluster model of crystalline aluminum. This yields a $MnAl_{12}Al_6$ cluster representing the local crystal environment of the impurity up to second-nearest neighbors. The Mn d orbitals overlap and hybridize with the surrounding Al p orbitals of the otherwise unoccupied $2t_{2g}$ orbital of pure aluminum in Fig. 3, resulting in the occupied, spatially

localized $t_{2g}(\epsilon_F)$ molecular orbital shown in Fig. 9. The net overlap of Al $p\pi$ bonding atomic orbitals in the $t_{1u}(\epsilon_F)$ orbital, argued above to be essential for superconductivity, is decreased around the Mn impurity due to the absence of localized p orbitals on Mn, as shown in the contour map of Fig. 10 [cf. Fig. 6], and there is a competition between the $t_{2g}(\epsilon_F)$ and $t_{1u}(\epsilon_F)$ orbitals for electrons. These effects tend to degrade the superconducting state by perturbing its long-range coherency, and the degrading effect will increase with the concentration of impurities. Mn impurities in aluminum, while not producing permanent magnetic moments below the Kondo temperature, $T_K \sim 900^\circ\text{K}$, give rise to localized spin fluctuations.⁵¹ The competition of the degenerate localized $t_{2g}(\epsilon_F)$ $d\sigma$ and extended $t_{1u}(\epsilon_F)$ $p\pi$ molecular orbitals for electrons at the Fermi energy, leading to fluctuations in orbital occupancy, implies a competition between the tendency to form local magnetic moments and the tendency to form the coherent spatially extended molecular state necessary for superconductivity.

It is also possible for molecular orbitals of the unperturbed coherent bonding type essential for superconductivity and orbitals of the localized antibonding type associated with local magnetic moments or collective magnetism to be practically degenerate at the Fermi energy. This could lead to a competition between superconductivity and magnetism as a sensitive function of orbital occupancy, which would depend on temperature according to Fermi statistics and/or on pressure according to orbital ordering. Such a situation might explain the rare incidence or "coincidence" of superconductivity and magnetism in the same material, e.g., chromium which is antiferromagnetic at ordinary pressure and superconducting at high pressure⁵⁰ (see discussion below) and superconducting molybdenum sulfides $\text{RE}_x\text{Mo}_6\text{S}_8$ (Chevrel compounds) containing a high concentration ($x \sim 1$) of magnetic rare-earth (RE) ions.⁵² A preliminary molecular-orbital analysis of the

Mo_6S_8 octahedral cluster which is the key structural unit in the superconducting Chevrel phases has been carried out, using the results of recent SCF- $X\alpha$ -SW studies of similar Mo-atom cluster compounds by Cotton and Stanley.⁵³ This analysis suggests that the superconducting state of these Chevrel phases and the more common ones not containing RE ions⁵⁴ arises exclusively from coherent spatially delocalized d-orbital bonding between the Mo atoms, promoted in part by the direct covalent overlap between Mo d orbitals in the Mo_6S_8 clusters and in part by the antibonding contribution of the interaction between Mo d orbitals and S ligand p orbitals. The latter contribution may be compared with the above-described effect of the $p\sigma^*$ -antibonding component of aluminum in promoting coherent spatially extended $p\pi$ bonding (see Figs. 5 through 7). On the other hand, the magnetic properties of the $\text{RE}_x\text{Mo}_6\text{S}_8$ compounds are associated exclusively with localized f orbitals on the RE ions which are formally but weakly antibonding with respect to the Mo_6S_8 clusters. Thus the interaction between the magnetic RE ions and the superconducting electrons is weak, explaining why the presence of such ions does not generally destroy the superconductivity of the Chevrel phases. More detailed SCF- $X\alpha$ -SW molecular-orbital studies of these systems are planned.

As a somewhat simpler illustration of the way the d orbitals of transition metals combine to form a coherent spatially extended superconducting state, consider the A15 compounds,⁵⁵ of which Nb_3Sn is the prime example. In this compound, the Nb atoms form a network of chains throughout the crystal, with the Sn atoms located at the corners and center of the unit cell. SCF- $X\alpha$ -SW cluster molecular-orbital studies reveal the presence of $d\delta$ -bonding molecular orbitals along the Nb chains at the Fermi energy. The $d\delta$ -bonding configuration is shown for four atoms of a chain in Fig. 11 and is consistent with the type of coherent wavefunction postulated above to be essential for the

superconducting state. A perspective drawing of $d\delta$ bonding along a chain of atoms is shown in Fig. 12. Like the preceding example of the Chevrel phases, the $d\delta$ bonding along the Nb chains is promoted partially by the direct covalent overlap between Nb d orbitals (note that the Nb-Nb interatomic distance in Nb_3Sn is less than that in elemental crystalline niobium) and partially by the interaction between Sn and Nb atoms. The influence of the Sn atoms on Nb-Nb bonding is analogous to that of the Cl ligands on Mo-Mo bonding in the molecular transition-metal coordination complex $Mo_2Cl_8^{4+}$, where the Mo-Mo bond distance is likewise shorter than that in crystalline metallic molybdenum.⁵⁶ This type of ligand-metal interaction is a significant contributing factor to the variation of T_c , which is proportional to metal-metal δ -bond overlap, among the superconducting A15 compounds. It has been customary to estimate T_c values for such compounds using the BCS formula (1) and the total density of states at the Fermi energy, $N(\epsilon_F)$, derived from band-structure calculations.⁵⁷ The occupied d bands of the A15 compounds can generally be partitioned into $d\sigma$, $d\pi$, and $d\delta$ bonding components in order of increasing energy toward the Fermi energy, with $d\delta^*$, $d\pi^*$, and $d\sigma^*$ antibonding components lying above the Fermi energy. However, the $d\sigma$ and $d\pi$ components do not correspond to coherent spatially extended wavefunctions of the type argued above to be necessary for superconductivity and therefore should be completely neglected when calculating $N(\epsilon_F)$ to estimate T_c .

The d bands of elemental transition metals can also be reconstructed in terms of overlapping σ -, π -, δ -bonding and δ^* -, π^* -, σ^* -antibonding cluster molecular-orbital components and the position of Fermi energy with respect to these components used as a simple gauge of whether the metal is likely to be a superconductor, magnet, or neither of these. For example, the transition metals in the vanadium column of the periodic table, which

correspond to a valence-electron-to-atom ratio $e/a = 5$, are superconducting with relatively high transition temperatures, V ($T_c = 5.38^\circ\text{K}$), Nb ($T_c = 9.50^\circ\text{K}$), and Ta ($T_c = 4.48^\circ\text{K}$), because the Fermi energy intersects the lower half of the d band where there are significant bonding (e.g., $d\delta$) components having the coherent spatial character necessary for superconductivity. In other words, for these elements the $d\delta$ orbital contribution to the density of states at the Fermi energy is large. On the other hand, although the second- and third-row transition metals in the chromium column of the periodic table (corresponding to $e/a = 6$) are also superconductors, their transition temperatures are relatively small, Mo ($T_c = 0.92^\circ\text{K}$) and W ($T_c = 0.012^\circ\text{K}$), because the Fermi energy intersects the d band near its center where the $d\delta$ orbital density of states is small. This type of analysis explains the variation of T_c for transition metals (and their alloys) with electron-to-atom ratio first pointed out by Matthias.³ Chromium itself is normally antiferromagnetic and becomes superconducting only at higher than normal pressure.⁵⁰ The incidence of both antiferromagnetism and superconductivity in Cr can be explained by an argument somewhat analogous to that presented above for the coexistence of magnetic rare-earth ions and superconductivity in the Chevrel phases. If the Fermi energy passes through the center of the Cr d band where spatially extended bonding orbitals of the type necessary for superconductivity and spatially localized antibonding orbitals of the kind associated with magnetism, i.e., the bonding and antibonding d-band "edges" respectively, are close in energy, then the orbital occupancy and dominant electronic state can be a sensitive function of interatomic distance. Spin-unrestricted SCF- $X\alpha$ -SW cluster molecular-orbital studies of Cr for an interatomic distance corresponding to normal pressure do indeed indicate spin-polarized antibonding d orbitals at the Fermi energy and spins of alternating sign or neighboring atoms, consistent with the antiferromagnetic

state.⁵⁸ Similar studies of Cr for interatomic distances corresponding to high pressures are in progress.

Toward the right of the periodic table, the ferromagnetism of the first-row transition metals (Fe, Co, and Ni) is associated with the Fermi energy coinciding with spin polarized $d\sigma^*$ - and $d\pi^*$ -antibonding molecular orbitals of the type shown in Fig. 1.^{33,37} On the other hand, preliminary theoretical studies suggest that the second- and third-row transition metals, Ru and Os, in the Fe column of the periodic table are superconducting, rather than ferromagnetic, because their hexagonal close-packed local molecular coordination is associated with coherent spatially extended bonding d orbitals, instead of incoherent spatially localized antibonding d orbitals, at the Fermi energy. The second-row transition metal, Pd, in the Ni column of the periodic table is neither superconducting nor ferromagnetic in its pure crystalline form but is strongly exchange enhanced by magnetic spin fluctuations.⁵⁹ SCF- $X\alpha$ -SW molecular-orbital studies of 19-atom palladium clusters representing the local crystalline environment up to second-nearest neighbors indicate the presence of degenerate spin-polarized $dd\pi^*$ and $pd\sigma^*$ antibonding orbitals at the Fermi energy.⁶⁰ Fluctuations of electron occupancy between these two types of orbitals are the discrete cluster analogues of the observed magnetic spin fluctuations. SCF- $X\alpha$ -SW cluster molecular-orbital studies of the interstitial alloy, palladium hydride (PdH),⁶¹ and palladium films containing radiation-induced defects,⁶² both of which are superconducting with $T_c \sim 3^\circ\text{K}$ or greater, are in progress. Preliminary results⁶³ suggest that the interstitial hydrogen and defects in palladium alter the spatial nature of the molecular orbitals at the Fermi energy, thereby quenching the spin fluctuations and inducing the superconducting state.

The above types of theoretical studies can also be used to explain why

some metals in the periodic table are neither superconducting nor magnetic. Among these, the noble metals Cu, Ag, and Au have been the subject of much discussion concerning the possibility of observing superconductivity at extremely low temperatures.⁶⁴ SCF- $X\alpha$ -SW studies of a 19-atom copper cluster representing bulk crystalline copper³⁵ suggest that superconductivity is unlikely to occur at any temperature (or reasonable pressure). The Fermi energy coincides with a molecular orbital of a_{1g} "spherical" symmetry which is primarily of the $s\sigma^*$ -antibonding type and which therefore lacks the coherent extended spatial character necessary for superconductivity (see Fig. 4 of Ref. 35 for a picture of this orbital). While there is some antibonding d-orbital contribution to this orbital due to the hybridization effect of the filled d band below the Fermi energy, it is too small and diffuse to give rise to localized or collective magnetic moments in pure copper. The only orbital that is capable, in principle, of forming a superconducting state in copper is an unoccupied t_{1u} $p\pi$ - $p\sigma^*$ orbital of the type shown above (Fig. 7) to be occupied at the Fermi energy in aluminum and responsible for its superconducting state. Thus the question of superconductivity in copper depends on whether this type of orbital, which lies well above the Fermi energy, can be brought into coincidence with the Fermi energy by any practically attainable pressure. Similar arguments are applicable to silver and gold.

While emphasis in this paper, thus far, has been placed on materials where the superconducting state is determined mainly by $p\pi$ or $d\delta$ bonding components, other types of chemical bonding, although less common, can also lead to coherent spatially extended wavefunctions of the kind necessary for superconductivity. For example, SCF- $X\alpha$ -SW cluster molecular-orbital models for superconducting "layered-structure" transition-metal compounds⁶⁵ such

as NbS_2 , TaS_2 , NbSe_2 , and TaSe_2 indicate that the Fermi energy is coincident with molecular orbitals of $d_{z^2}(a_1'^*)$ symmetry, shown schematically in Fig. 13 for three neighboring metal atoms in a single layer.⁶⁶ This orbital is moderately antibonding between the transition-metal d orbitals and chalcogen "ligand" p orbitals (not shown in Fig. 13) but weakly bonding between the "doughnut-like" annular regions of the metal d_{z^2} orbitals in each layer (the dashed profiles shown in Fig. 13), in agreement with the chemical-bonding model of Krebs.¹⁵ The bonding between annular regions forms a diffuse but spatially coherent wavefunction throughout each layer, thereby satisfying the orbital criterion for the existence of superconductivity. In this respect, the superconducting state of the layered transition-metal dichalcogenides is "two-dimensional." However, the total superconducting state of the crystal is a composite result of the three-dimensional array of layered d_{z^2} orbitals, just as the superconducting states of aluminum and A15 compounds discussed above are the composite results of three-dimensional networks of "quasi-one-dimensional" $p\pi$ and $d\delta$ orbital configurations. The relatively low transition temperatures of these layered superconductors, e.g., NbS_2 ($T_c = 6^\circ\text{K}$) and TaSe_2 ($T_c = 0.2^\circ\text{K}$), as compared with those of the $d\delta$ -bonded A15 compounds, e.g., Nb_3Sn ($T_c = 18^\circ\text{K}$) and V_3Sn ($T_c = 3.8^\circ\text{K}$), are consistent with the fact that the bond overlap between the annular parts of the d_{z^2} orbitals in the former compounds (see Fig. 13) is significantly less than that between the $d\delta$ orbitals in the latter compounds (see Fig. 12). The exact amounts of bond overlap and concomitant T_c values for the layered superconductors are dependent on the antibonding contributions of the chalcogen ligand p orbitals to the $d_{z^2}(a_1'^*)$ molecular orbitals, in much the same fashion as the $p\pi$ bonding orbital components in aluminum are promoted by the $p\sigma^*$ antibonding components (see Figs. 5 through 7), and in much the same way as the net $d\delta$ bonding along the chains of metal atoms in the A15 compounds, Nb_3Sn and V_3Sn ,

is dependent on the interaction of the metal atoms with the neighboring Sn ligands. The intercalation of organic molecules, such as pyridine, between the layers of superconducting transition-metal dichalcogenides does not appreciably alter their T_c values.⁶⁵ This is explained by the fact that the bonding between the layers and intercalate molecules occurs via the d_{z^2} lobes perpendicular to each layer (the solid orbital contours in Fig. 13), which leaves largely unaffected the bonding between annular regions within each plane (the dashed orbital contours in Fig. 13) responsible for the superconducting state. The weak annular type of bonding between d_{z^2} orbitals is not strictly limited to layered transition-metal compounds but can also contribute, along with the more dominant $d\delta$ bonding, to the superconducting state in transition metals and their alloys.

In principle, spherically symmetric s orbitals can also overlap to form coherent spatially extended σ -type bonding molecular orbitals like that shown schematically in Fig. 14 and thus can lead to the superconducting state. However, it is unusual to find materials where this kind of s-orbital bonding occurs at the Fermi energy. It is more common for $s\sigma$ bonding orbitals to have energies well below the Fermi energy, e.g., the $1a_{1g}$ cluster molecular orbitals and $\Gamma_1(\vec{k}=0)$ Bloch eigenstates of aluminum (Fig. 3), copper (Fig. 1 of Ref. 35), and lithium (Fig. 3 of Ref. 67). As discussed above, the molecular orbitals at the Fermi energy in copper at normal pressure are $s\sigma^*$ antibonding orbitals which cannot lead to the superconducting state, whereas $p\pi$ bonding orbital components at the Fermi energy are responsible for the superconducting state of aluminum. The absence of $s\sigma$ or $p\pi$ bonding orbitals at the Fermi energy of lithium⁶⁷ explains the nonsuperconducting state of this and similar alkali metals at normal pressures. Nevertheless, preliminary SCF-X α -SW cluster molecular-orbital models for PdH_x suggest that diffuse $s\sigma$

bond overlap of the kind shown in Fig. 14 occurs at the Fermi energy between interstitial hydrogen atoms, under the chemical influence of neighboring palladium atoms, for large concentrations ($x \sim 1$) of hydrogen and may play a key role in determining the superconducting state of PdH.⁶³

Finally, while the coherent spatially extended bonding of f orbitals has not been addressed in this paper, their possible contribution to the superconducting states of transuranium elements at normal and high pressure are currently under theoretical investigation.

IV. CONCLUSIONS

Evidence has been presented in this paper that a material is likely to be a superconductor if the electronic states at the Fermi energy, defined by the highest occupied molecular orbitals calculated by the SCF- $X\alpha$ -SW method for clusters representing the local molecular environment in the material, have coherent spatially extended (e.g., $p\pi$, $d\delta$, d_{z^2} , or $s\sigma$) bonding components. It has also been shown that, while these individual orbital components are usually "one-dimensional" or "two-dimensional" in nature (see Figs. 8, 12, 13, and 14), the composite superconducting state of the material arises from the coherent three-dimensional "network" or "array" of these components. Moreover, it has been shown that for each such orbital component, covalent bond overlap in a line or plane of atoms is promoted by the antibonding repulsion of atoms not in that line or plane, as exemplified by the $p\pi$ - $p\sigma^*$ interaction in aluminum (see Figs. 5 through 7) and by the ligand-metal interactions in transition-metal compounds. This results in the type of "rigid" or "frozen" wavefunction of wide spatial extent originally postulated by London⁸ and Slater⁹ to be necessary for the production of nondissipative diamagnetic currents. These orbital criteria

can be used to explain simply and directly observed chemical trends of superconductors (e.g., trends of T_c with chemical bonding), to rule out certain types of substances as possible superconductors, and to suggest ways of systematically improving existing classes or synthesizing new classes of superconducting materials.

For example, it has been suggested that certain types of organic molecules or polymers of more or less one-dimensional structure with conjugated bonds might not only be superconducting but could possibly persist in this state at room temperature and higher.¹⁰ Since three-dimensionality seems to be essential for the stability or "rigid" character of the superconducting state, superconductivity of any kind and most certainly high T_c superconductivity in truly one-dimensional systems can be ruled out. Furthermore, while the highest occupied molecular orbitals in most conjugated organic molecules are π orbitals associated with the carbon p electrons, they are typically of the π_2 and π_3 symmetries illustrated for benzene in Fig. 2. Such orbitals have nodes along the bond direction, e.g., the phase of the wavefunction changes, and therefore lack the spatial coherency necessary for superconductivity. These conditions are encountered, for instance, in the much studied tetrathiafulvalene (TTF)-tetracyanoquinodimethane (TCNQ) system.⁶⁸ Although this substance in crystalline form exhibits a high degree of ordinary electrical conductivity along a certain crystallographic direction related to the one-dimensional stacking of the TTF and TCNQ molecules, SCF- $X\alpha$ -SW studies indicate that the π molecular orbitals near the Fermi energy have nodal structures which are the antithesis of the coherent spatial character essential for the existence of the superconducting state.⁶⁹ Thus the possibility of superconductivity in TTF-TCNQ is ruled out from first principles.

On the other hand, crystalline polymeric sulfur nitride (SN_x) is not

only a good ordinary electrical conductor along the direction of "fiber bundles" formed by large aggregates of individual polymer molecules, but is also an anisotropic superconductor, albeit a low T_c ($\sim 0.25^\circ\text{K}$) one.⁷⁰ SCF- $X\alpha$ -SW studies reveal that the Fermi energy is coincident with coherent $p\pi$ bonding molecular orbitals spatially delocalized along the $(\text{SN})_x$ polymeric chains.⁷¹ Despite the effectively one-dimensional character of these $p\pi$ orbitals, they lead to a reasonably stable or "rigid" superconducting state for each fiber as a result of $p\pi$ interchain coupling in the (100) plane and $p\sigma$ interchain coupling in the $(\bar{1}02)$ plane,⁷¹ These orbitals are therefore somewhat analogous to the $p\pi$ - $p\sigma^*$ molecular orbitals shown earlier (see Figs. 5 through 7) to be responsible for the superconducting state of aluminum. However, in $(\text{SN})_x$ the $p\pi$ components lie exclusively along the direction of the fibers and thus lead to anisotropic superconductivity, whereas in aluminum there are three equivalent $p\pi$ components along the three principal cubic crystallographic directions which lead to isotropic superconductivity. The $p\pi$ anisotropy and relatively weak $p\pi$ bond overlap associated with the "zig-zag" structure of the $(\text{SN})_x$ polymers are most likely responsible for the relatively low transition temperature of this material. The element phosphorus, which is closely related to sulfur and nitrogen, becomes metallic and superconducting for moderate pressure where its crystal structure is cubic.⁷² SCF- $X\alpha$ -SW cluster molecular-orbital studies of cubic phosphorus suggest that for an interatomic distance corresponding to this pressure the highest occupied molecular orbitals have coherent $p\pi$ bonding character along chains of phosphorus atoms which are coupled in a three-dimensional network of $p\pi$ orbital components by the interchain interactions.⁷³ This type of bonding is responsible for the superconducting state of phosphorus (under pressure), just as it is for $(\text{SN})_x$ and aluminum. The

relatively high transition temperature ($T_c \sim 6^\circ\text{K}$) for phosphorus is due to the fact that the cubic structure under pressure promotes coherent $p\pi$ bond overlap. This suggests that the transition temperature of $(\text{SN})_x$ would be raised, in principle, if it could be crystallized in a structure of higher three-dimensional symmetry which would also promote $p\pi$ bond overlap.

The above observations provide strong theoretical support for Matthias^{3,74} arguments that the highest transition temperature for a particular type of superconducting material will occur in the structural modification of highest symmetry. These observations also suggest that in the quest for higher T_c superconductors, it would be more profitable in the long run to attempt to optimize systematically, through structural or compositional modification (e.g., alloying or compound formation), the individual chemical bonding (e.g., $p\pi$, $d\delta$, etc.) components of high-symmetry materials. For example, the existence of high T_c superconducting Chevrel phases⁵⁴ discussed above, where the basic structural units are symmetrical clusters containing coherent metal-metal bonds, and the existence of small-particle superconductors with higher transition temperatures than the corresponding bulk materials^{5,6} suggest that other compounds or composite materials based on coherently bonded metal clusters could be potential superconductors of relatively high T_c .

One could go on and give many other examples where the above-described molecular-orbital criteria for superconductivity can consistently explain the chemical trends of known superconductors, e.g., intermetallic compounds, solid-solution alloys, and amorphous alloys, as well as suggesting new types of superconductors. However, such examples will be the subjects of future papers. It remains here to comment on only one more example where there has been much speculation on the possibility of superconductivity, namely

metallic hydrogen prepared at very high pressure.⁷⁵⁻⁷⁷ Preliminary SCF- $X\alpha$ -SW molecular-orbital models suggest that, while the electronic structure of solid hydrogen for high-pressure interatomic distances and crystal structure is consistent with metallic behavior, this substance is unlikely to be a superconductor. The Fermi energy coincides with an σ^* antibonding molecular orbital of the type already shown above to be responsible for the nonsuperconducting state of copper. Thus, as in the example of copper, the question of superconductivity in metallic hydrogen depends on whether an unoccupied spatially coherent $p\pi$ -bonding orbital, which lies well above the Fermi energy, can be brought into coincidence with the Fermi energy by any attainable pressure.

ACKNOWLEDGMENTS

KHJ is grateful to the National Science Foundation, Grant No. DMR-7818800, and to the Office of Naval Research for sponsoring this research. KHJ is also grateful to J. Sukkar for suggesting the interesting analogy between the real-space molecular-orbital description of the superconductors and the coherent transmission of light by optical fibers. KHJ is especially grateful to M. Sukkar for continued encouragement during the course of this research.

REFERENCES

1. J. Bardeen, L. N. Cooper, and J. R. Schrieffer, Phys. Rev. 108, 1175 (1957).
2. L. N. Cooper, Phys. Rev. 104, 1189 (1956).
3. B. T. Matthias, Phys. Rev. 97, 74 (1955); in Progress in Low Temperature Physics, Vol. II, edited by C. J. Gorter (North-Holland, Amsterdam, 1957), p. 138; in The Science and Technology of Superconductivity, Vol. 1, edited by W. D. Gregory, W. N. Matthews, Jr., and E. A. Edelsack (Plenum, New York, 1973), p. 263; Physica 55, 69 (1971).
4. W. L. Johnson, S. J. Poon, and P. Duwez, Phys. Rev. B11, 150 (1975).
5. S. Matsuo, H. Sugiura, and S. Noguchi, J. Low Temp. Phys. 15, 481 (1974).
6. K. Ohshima, T. Kuroshi, and T. Fujita, J. Phys. Soc. Japan 41, 1234 (1976).
7. F. London, and H. London, Proc. Roy. Soc. A149, 71 (1935); Physica 2, 341 (1935); F. London, Proc. Roy. Soc. A152, 24 (1935).
8. F. London, Superfluids, Vol. 1 (Wiley, New York, 1950).
9. J. C. Slater, Phys. Rev. 51, 195 (1937); 52, 214 (1937).
10. W. A. Little, Phys. Rev. 134, A1416 (1964).
11. D. W. Allender, J. M. Bray, and J. Bardeen, Phys. Rev. B7, 1020 (1973); Phys. Rev. B8, 4433 (1973).
12. J. J. Hopfield, Phys. Rev. 186, 443 (1969).
13. D. M. Gualtieri, J. Appl. Phys. 45, 1880 (1974).
14. C. M. Varma and R. C. Dynes, in Superconductivity in d- and f-Band Metals, edited by D. H. Douglas (Plenum, New York, 1976), p. 507.
15. H. Krebs, Prog. in Solid State Chem. 9, 269 (1975).
16. J. C. Slater and K. H. Johnson, Phys. Rev. B5, 844 (1972); K. H. Johnson and F. C. Smith, Jr., Phys. Rev. B5, 831 (1972); J. C. Slater and K. H. Johnson, Physics Today 27, 34 (1974).

17. J. C. Slater, in Advances in Quantum Chemistry, Vol. 6, edited by P.-O. Löwdin (Academic, New York, 1972); The Self-Consistent Field for Molecules and Solids, Vol. 4 of Quantum Theory of Molecules and Solids (McGraw-Hill, New York, 1974).
18. K. H. Johnson, *J. Chem. Phys.* 45, 3085 (1966); in Advances in Quantum Chemistry, Vol. 7, edited by P.-O. Löwdin (Academic, New York, 1973), p. 143.
19. K. H. Johnson, J. G. Norman, Jr., and J. W. D. Connolly, in Computational Methods for Large Molecules and Localized States in Solids, edited by F. Herman, A. D. McLean, and R. K. Nesbet (Plenum, New York, 1973), p. 161.
20. K. H. Johnson, in Annual Review of Physical Chemistry, Vol. 26, edited by H. Eyring, C. J. Christensen, and H. S. Johnston (Annual Reviews, Palo Alto, California, 1975), p. 39.
21. F. A. Cotton, E. E. Hazen, Jr., V. W. Day, S. Larsen, J. G. Norman, Jr., S. T. K. Wong, and K. H. Johnson, *J. Am. Chem. Soc.* 95, 2367 (1973).
22. C. Y. Yang, K. H. Johnson, R. H. Holm, and J. G. Norman, Jr., *J. Am. Chem. Soc.* 97, 6596 (1975).
23. B. H. Huynh, D. A. Case, and M. Karplus, *J. Am. Chem. Soc.* 99, 6103 (1977); D. A. Case and M. Karplus, *J. Am. Chem. Soc.* 99, 6182 (1977); D. A. Case, B. H. Huynh, and M. Karplus, *J. Am. Chem. Soc.* (in press).
24. K. H. Johnson, F. Herman, and R. Kjellander, in Electronic Structure of Polymers and Molecular Crystals, edited by J.-M. Andre, J. Ladik, and J. Delhalle (Plenum, New York, 1975), p. 601.
25. R. P. Messmer, in Theoretical Chemistry, Vol. 1, edited by A. D. Buckingham, and C. A. Coulson (Butterworths, London, 1975), p. 217.
26. K. H. Johnson, *Crit. Rev. Solid State and Mat. Sci.* 7, 101 (1978).

27. R. P. Messmer, in The Nature of the Surface Chemical Bond, edited by T.-N. Rhodin and G. Ertl (North Holland, Amsterdam, 1979), p. 51.
28. G. D. Watkins and R. P. Messmer, *Phys. Rev. Lett.* 32, 1244 (1974).
29. B. G. Cartling, *J. Phys. C.* 8, 3171; 3183 (1975).
30. L. A. Hemstreet, *Phys. Rev.* B15, 834 (1977).
31. A. Fazzio, J. R. Leite, and M. L. DeSiqueira, *J. Phys. C.* 11, L175 (1978); 12, 513 (1979).
32. K. H. Johnson, H. J. Kolari, J. P. deNeufville and D. L. Morel, *Phys. Rev.* (submitted for publication).
33. R. P. Messmer, S. K. Knudson, K. H. Johnson, J. B. Diamond, and C. Y. Yang, *Phys. Rev.* B13, 1396 (1976).
34. D. R. Salahub and R. P. Messmer, *Phys. Rev.* B16, 2526 (1977).
35. K. H. Johnson, D. D. Vvedensky, and R. P. Messmer, *Phys. Rev.* B19, 1519 (1979).
36. T. E. Fischer, S. R. Kelemen, K. P. Wang, and K. H. Johnson, *Phys. Rev.* (submitted for publication).
37. C. Y. Yang, Ph.D. Thesis, Department of Materials Science and Engineering (Massachusetts Institute of Technology, June, 1977) (unpublished);
C. Y. Yang and K. H. Johnson, *Phys. Rev.* (manuscript in preparation).
38. R. P. Messmer and K. H. Johnson (unpublished work).
39. R. P. Messmer and D. R. Salahub, *Phys. Rev.* B16, 2526 (1977).
40. H. L. Yu, *Phys. Rev.* B15, 3609 (1977); *J. Chem. Phys.* 69, 1755 (1978).
41. J. W. Davenport, *Phys. Rev. Lett.* 36, 945 (1976).
42. R. P. Messmer, D. R. Salahub, and J. W. Davenport, *Chem. Phys. Lett.* 57, 29 (1978).
43. J. W. Davenport, W. Ho, and J. R. Schrieffer, *Phys. Rev.* B17, 3115 (1978).
44. R. P. Messmer and S. H. Lamson, *Chem. Phys. Lett.* (in press).

45. A. P. Ginsberg, *J. Am. Chem. Soc.* (in press).
46. J. C. Slater, Quantum Theory of Matter, Second Edition (McGraw-Hill, New York, 1968), p. 578.
47. F. London, *J. Phys. Radium* 8, 397 (1937).
48. R. C. Haddon, *J. Am. Chem. Soc.* 101, 1722 (1979).
49. J. C. Slater, The Self-Consistent Field for Molecules and Solids, Vol. 4 of Quantum Theory of Molecules and Solids (McGraw-Hill, New York, 1974), p. 117.
50. C. Kittel, Introduction to Solid State Physics, 5th Edition (Wiley, New York, 1976), Chapter 12.
51. G. Grüner, *Adv. Phys.* 23, 941 (1974).
52. Ø. Fischer, A. Treyvaud, R. Chevrel, and M. Sergent, *Solid State Comm.* 17, 721 (1975).
53. F. A. Cotton and G. G. Stanley, *Chem. Phys. Lett.* 58, 450 (1978).
54. B. T. Matthias, M. Murezio, E. Corenzwit, A. S. Cooper, and H. E. Barz, *Science* 175, 1465 (1972).
55. R. A. Hein, in The Science and Technology of Superconductivity, Vol. 1, edited by W. D. Gregory, W. N. Matthews, Jr., and E. A. Edelsack (Plenum, New York, 1973), p. 333.
56. J. G. Norman, Jr., and H. J. Kolari, *J. Chem. Soc. Chem. Commun.* 303 (1974); *J. Am. Chem. Soc.* 97, 33 (1975).
57. B. M. Klein, L. L. Boyer, and D. A. Papaconstantopoulos, *Phys. Rev. Lett.* 42, 530 (1979); B. M. Klein, L. L. Boyer, D. A. Papaconstantopoulos, and L. F. Mattheis, *Phys. Rev.* B18, 6411 (1978).
58. D. R. Salahub and R. P. Messmer (unpublished work).

59. G. Gladstone, M. A. Jensen, and J. R. Schrieffer, in Superconductivity, edited by R. D. Parks (Marcel Dekker, New York, 1969), Vol. 2.
60. D. D. Vvedensky, Ph.D. Thesis, Department of Materials Science and Engineering (Massachusetts Institute of Technology, August, 1979) (unpublished).
61. F. A. Lewis, The Palladium/Hydrogen System (Academic, New York, 1967).
62. B. Stritzker, Phys. Rev. Lett. 42, 1769 (1979).
63. D. D. Vvedensky and K. H. Johnson (unpublished work).
64. B. T. Matthias, Int. J. Quantum Chem. 6S, 429 (1972).
65. F. R. Gamble, F. J. DiSalvo, R. A. Klemm, and T. H. Geballe, Science 168, 568 (1970).
66. V. W. Day and K. H. Johnson (unpublished work).
67. J. G. Fripiat, K. T. Chow, M. Boudart, J. B. Diamond, and K. H. Johnson, J. Molec. Catal. 1, 59 (1975/76).
68. See review articles by A. N. Bloch; R. Comes; A. J. Heeger, D. Jerome, and M. Weger; and J. Torrance, in Chemistry and Physics of One-Dimensional Metals, edited by H. J. Keller (Plenum, New York, 1977).
69. F. Herman, D. R. Salahub, and R. P. Messmer, Phys. Rev. B16, 2453 (1977).
70. R. L. Greene and G. B. Street, in Ref. 68.
71. R. P. Messmer and D. R. Salahub, Chem. Phys. Lett. 41, 73 (1976);
D. R. Salahub and R. P. Messmer, Phys. Rev. 14, 2592 (1976).
72. J. Wittig and B. T. Matthias, Science 160, 994 (1968).
73. K. H. Johnson and J. G. Norman, Jr. (unpublished work).
74. B. T. Matthias, Int. J. Quantum Chem. 10S, 435 (1976).
75. N. W. Ashcroft, Phys. Rev. Lett. 21, 1748 (1968).
76. T. Schneider, Helv. Phys. Acta 42, 957 (1969).
77. V. L. Ginzburg, Physica 55, 207 (1971).

FIGURE CAPTIONS

Fig. 1. Contour map of the highest occupied "spin-up" molecular-orbital wavefunction of t_{2g} symmetry for a 15-atom iron cluster representing the local molecular environment, up to second-nearest neighbors, in bcc crystalline α -iron. The contours are plotted in the (110) plane containing four of the eight nearest neighbors and two of the six second-nearest neighbors. The solid and dashed contours represent positive and negative values, respectively, of the wavefunction, with the nodes between solid and dashed contours indicating $dd\sigma^*$ anti-bonding character between nearest neighbors and $dd\pi^*$ antibonding character between second-nearest neighbors. This spin-polarized t_{2g} wavefunction is the discrete cluster molecular-orbital analogue of states at the top of the majority-spin d band near the Fermi energy in ferromagnetic crystalline α -iron. See Refs. 26 and 37 for further details.

Fig. 2. Comparison between the real-space molecular-orbital and k-space band-structure representations of the $p\pi$ electronic states of a benzene molecule, based on the one-dimensional periodicity of the carbon atoms (see Ref. 46). The arrows denote the spin pairing and degeneracy of each molecular orbital and the "Fermi energy" ϵ_F separates the occupied states from the unoccupied ones.

Fig. 3. SCF- $X\alpha$ -SW molecular-orbital energy levels of a 19-atom aluminum cluster representing the local molecular environment, up to second-nearest neighbors, in fcc crystalline aluminum. The orbitals are labeled according to the irreducible representations of the O_h cluster symmetry group. The $4t_{1u}(\epsilon_F)$ level corresponds to the highest occupied cluster molecular orbital. Shown for comparison are the energy-band profiles for aluminum, plotted along principal

symmetry directions of the Brillouin zone.

Fig. 4. Electronic density of states for a 19-atom cluster representing the local molecular environment in crystalline aluminum, determined by a Gaussian broadening of the discrete molecular-orbital energy levels shown in Fig. 3. The arrow denotes the position of the Fermi energy. See Ref. 34 for details.

Fig. 5. Contour map of the highest occupied molecular-orbital wavefunction of t_{1u} symmetry for a 19-atom cluster representing the local molecular environment in crystalline aluminum. This orbital corresponds to the $4t_{1u}(\epsilon_F)$ energy level shown in Fig. 3. The contours are plotted in the (200) plane containing four of the twelve nearest neighbors and four of the six second-nearest neighbors. The solid and dashed profiles represent positive and negative values, respectively, of the wavefunction. Regions of net overlap between contours of the same sign are bonding, whereas regions of positive and negative contours separated by nodes are antibonding. Note the p_{π} bonding character along the "horizontal" direction and the complementary p_{σ^*} antibonding character along the "vertical" direction. Since this molecular orbital is triply degenerate, there are two other equivalent wavefunctions with p_{π} and p_{σ^*} components directed along orthogonal crystallographic directions, resulting in an isotropic orbital charge distribution.

Fig. 6. Contour map of the cluster molecular orbital shown in Fig. 5 but plotted in the (110) plane.

Fig. 7. Real-space molecular-orbital representation of the electronic states of crystalline aluminum at the Fermi energy, derived from the generalization of the $t_{1u}(\epsilon_F)$ cluster molecular-orbital configuration shown in Fig. 5 to include more shells of atoms. Note the coherent spatially extended $p\pi$ bonding character along the "horizontal" direction and the complementary $p\sigma^*$ antibonding character along the "vertical" direction. As in Figs. 5 and 6, the triple degeneracy of this molecular orbital implies two equivalent $p\pi$ - $p\sigma^*$ wavefunctions along orthogonal crystal directions, thereby resulting in an isotropic orbital charge distribution. This three-dimensional "network" of $p\pi$ and $p\sigma^*$ orbital components results in the type of "rigid" or "frozen" wavefunction of wide spatial extent originally postulated by London (Ref. 8) and Slater (Ref. 9) to be necessary for the superconducting state.

Fig. 8. Perspective drawing of spatially coherent $p\pi$ bonding molecular-orbital components along a line of atoms. The solid and dashed contours represent positive and negative values, respectively, of the wavefunction.

Fig. 9. Contour map of the highest occupied molecular-orbital wavefunction of t_{2g} symmetry for a 19-atom cluster representing the local molecular environment of an isolated substitutional Mn impurity in crystalline aluminum up to second-nearest neighbors. The contours are plotted in the (200) plane containing the Mn impurity, four of the twelve nearest-neighbor Al atoms, and four of the six second-nearest neighbor Al atoms. The solid and dashed contours represent positive and negative values, respectively, of the wavefunction. The σ -type chemical interaction between the four-lobe Mn d orbital and four nearest-neighbor Al p orbitals is clearly evident. Note

that this t_{2g} molecular orbital is unoccupied for pure aluminum in its superconducting ground electronic state (the $2t_{2g}$ level lying above the Al_{19} cluster Fermi energy in Fig. 3).

Fig. 10. Contour map of the highest occupied molecular-orbital wavefunction of t_{1u} symmetry for a 19-atom cluster representing the local molecular environment of an isolated substitutional Mn impurity in crystalline aluminum up to second-nearest neighbors. The contours are plotted in the same (110) plane as the corresponding orbital for pure aluminum in Fig. 6. Direct comparison of Fig. 10 and Fig. 6 reveals that the absence of localized p orbitals on the Mn atom at the cluster Fermi energy reduces the net overlap of Al $p\pi$ orbitals, thereby locally perturbing the coherency of the $p\pi$ bonding component and degrading the superconducting state.

Fig. 11. The spatially coherent $d\delta$ bonding component of the highest occupied molecular orbital for the A15 compound, Nb_3Sn , shown along four atoms of a Nb chain. The three-dimensional network of such $d\delta$ components, coupled with the Sn(ligand)-Nb(metal) interactions, is responsible for the superconducting state of Nb_3Sn and other A15 compounds.

Fig. 12. Perspective drawing of spatially coherent $d\delta$ bonding molecular-orbital components along a line of atoms. The solid and dashed contours represent positive and negative values, respectively, of the wavefunction.

Fig. 13. Perspective drawing in a plane of three atoms of spatially coherent d_{z^2} bonding molecular-orbital components of the type responsible for the highest occupied cluster molecular orbitals of layered transition-metal dichalcogenides (e.g., NbS_2). The spatially extended coherent bond overlap of the annular regions (the dashed

contours) of the d_{z^2} orbitals in each layer, coupled with the effects of Nb(metal)-S(ligand) interactions, is responsible for the superconducting state of such compounds.

Fig. 14. Perspective drawing of spatially coherent σ bonding molecular-orbital components along a line of atoms.

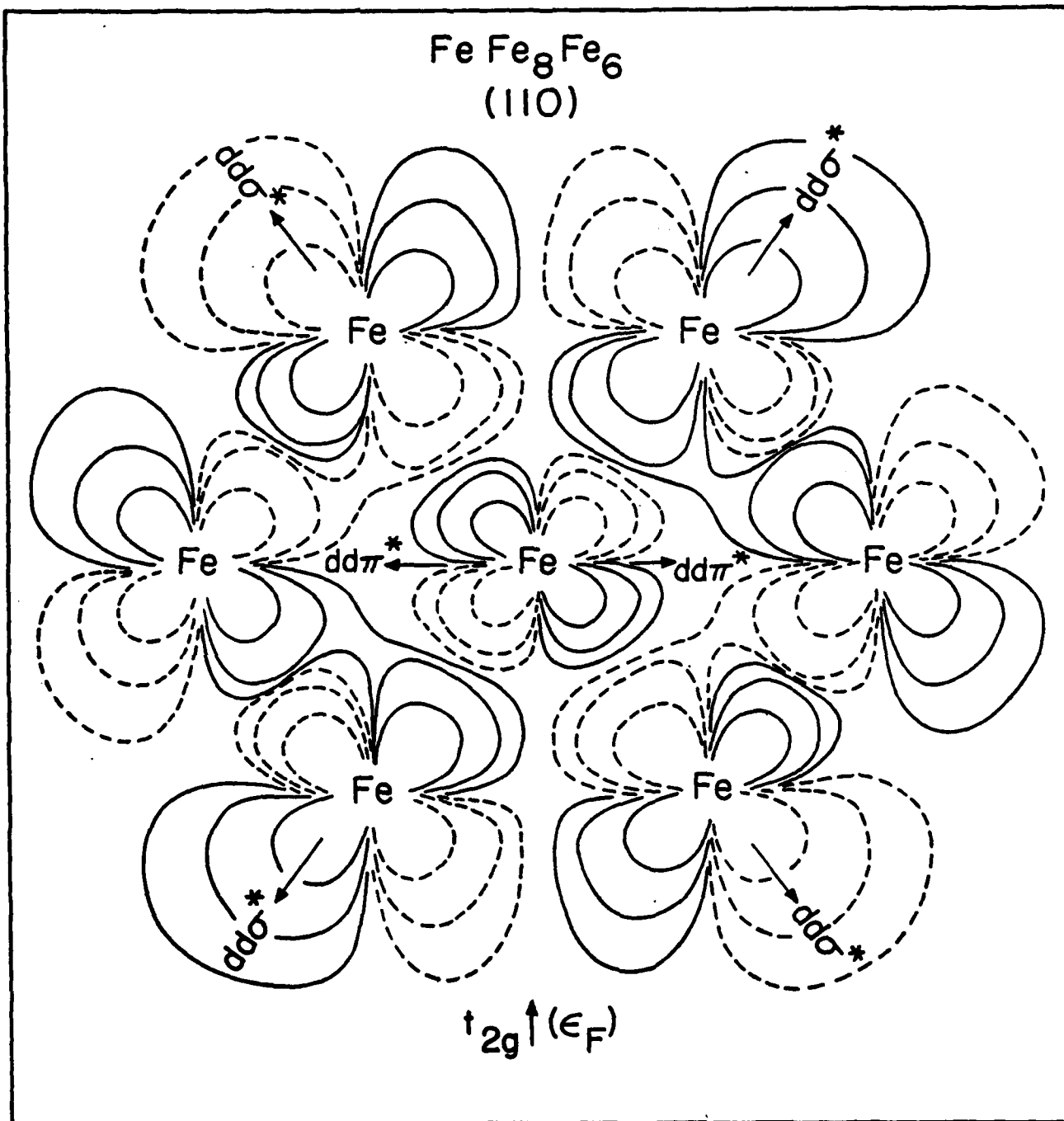


Figure 1

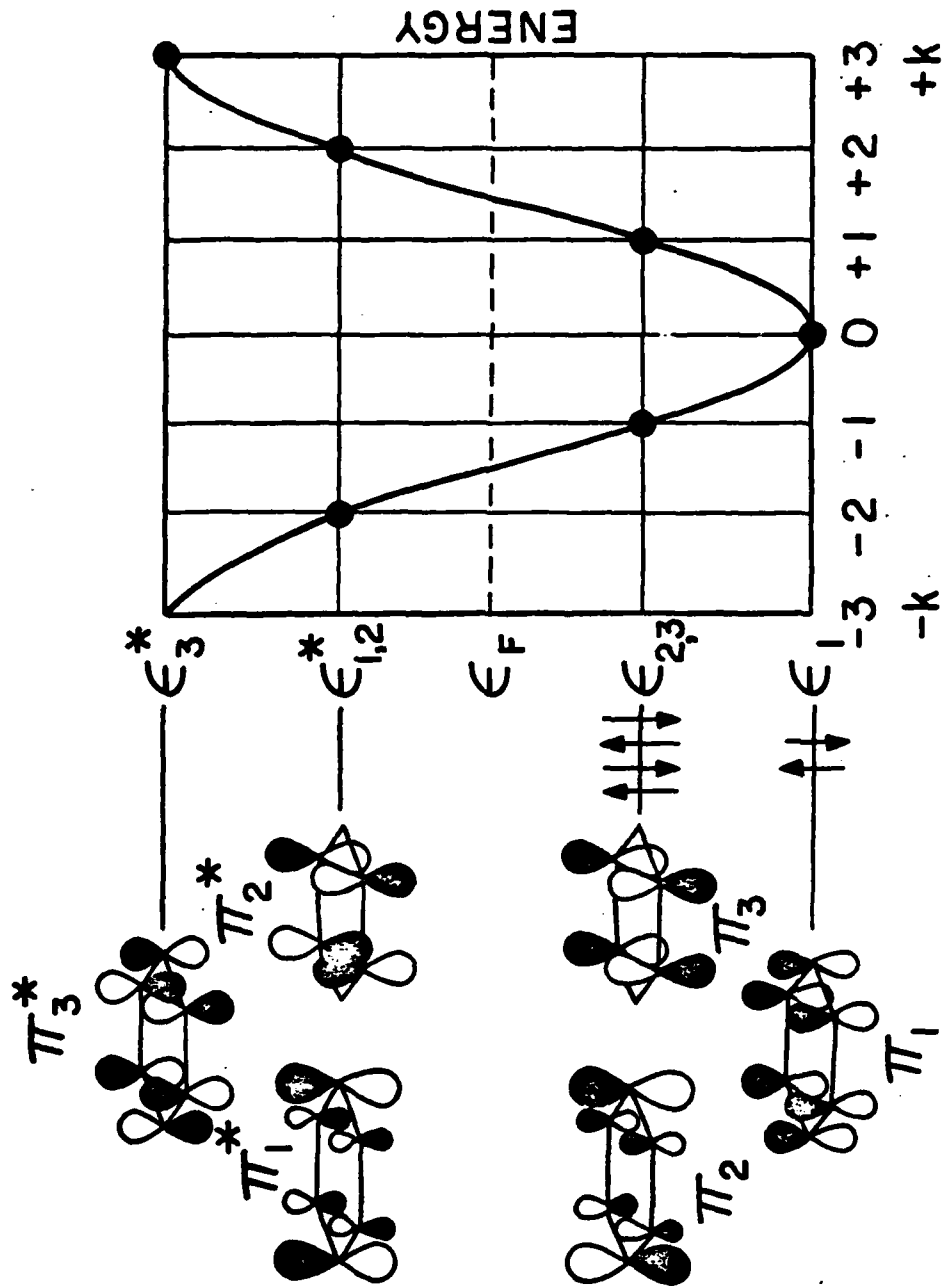


Figure 2

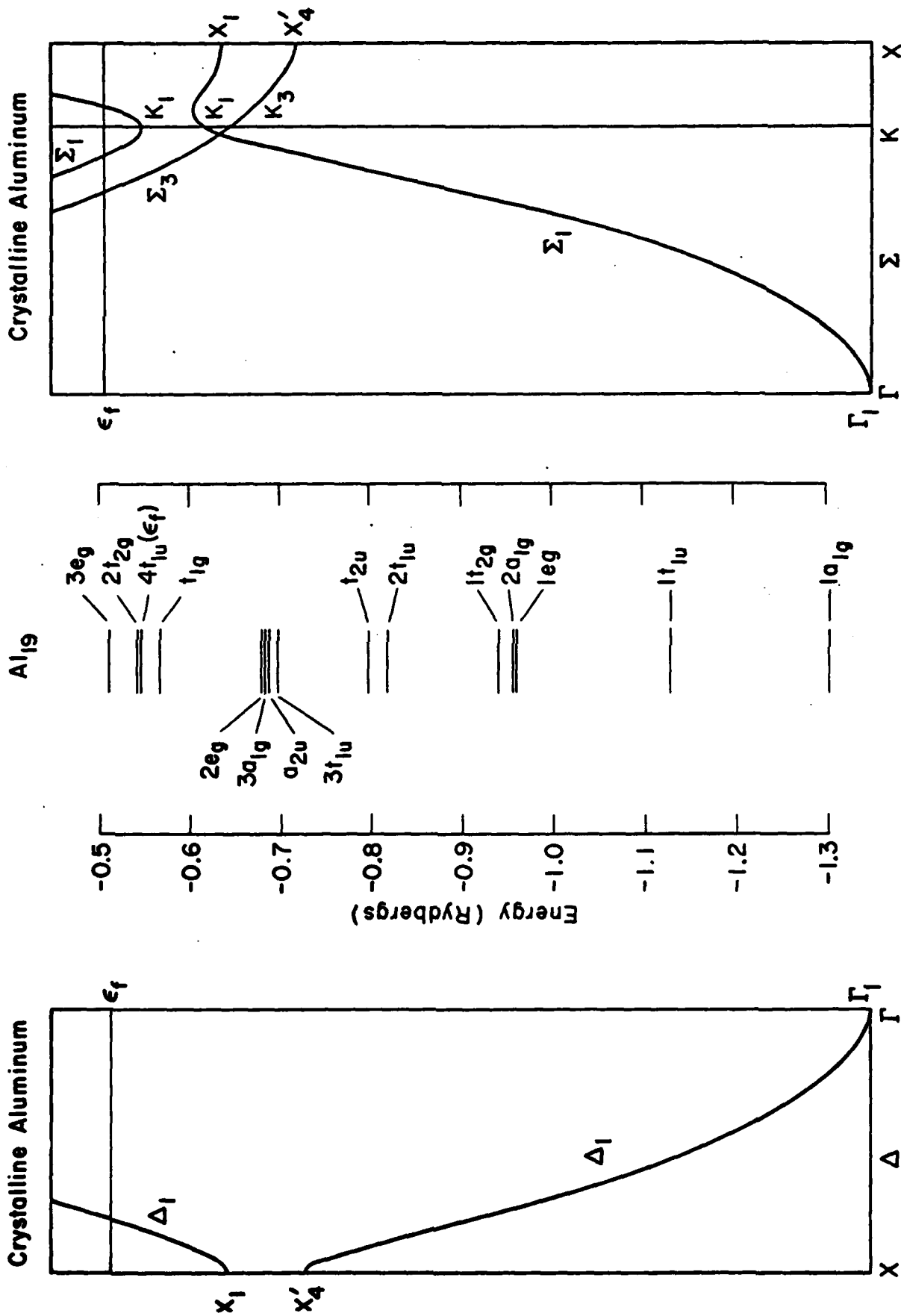


Figure 3

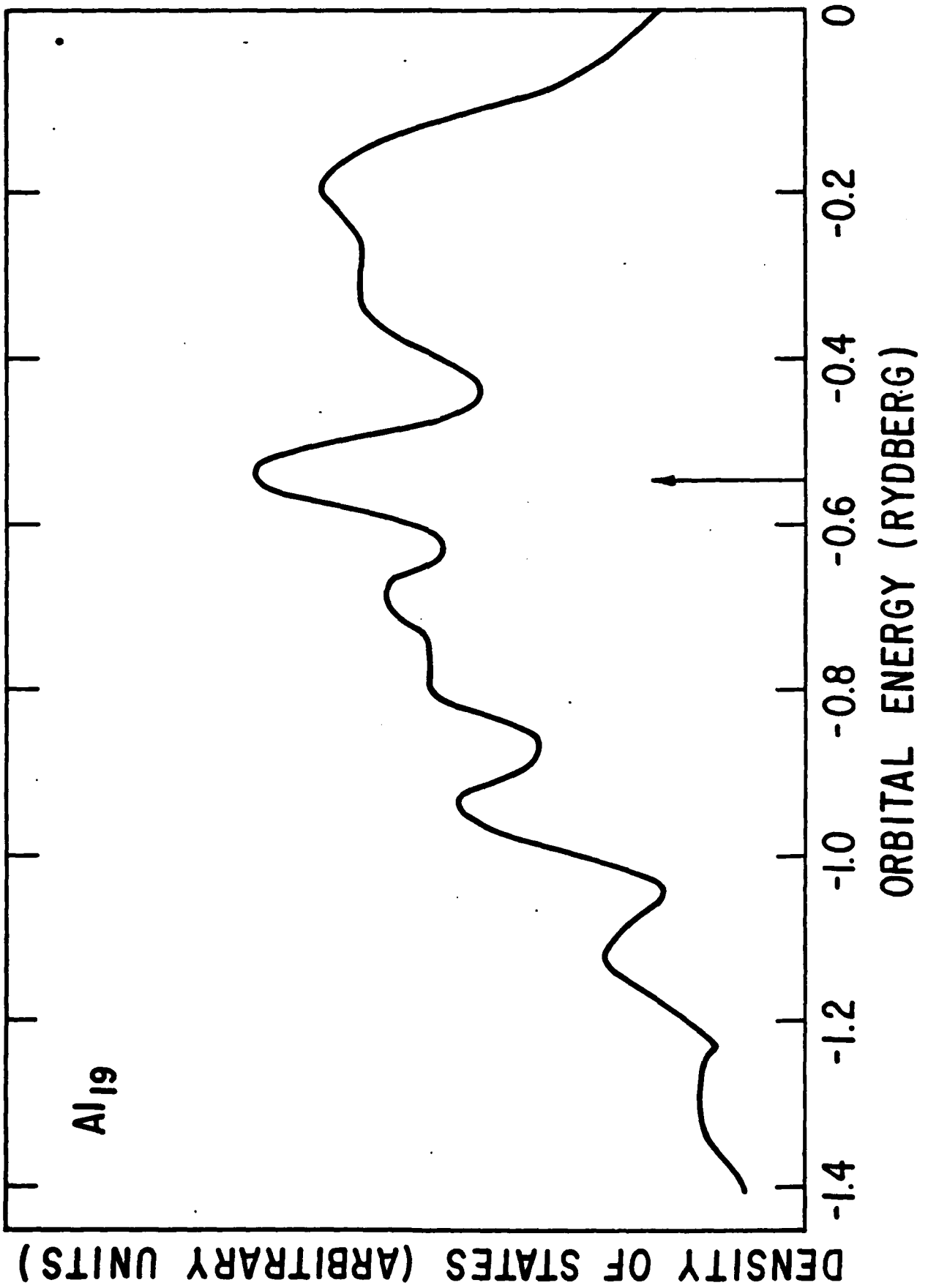


Figure 4

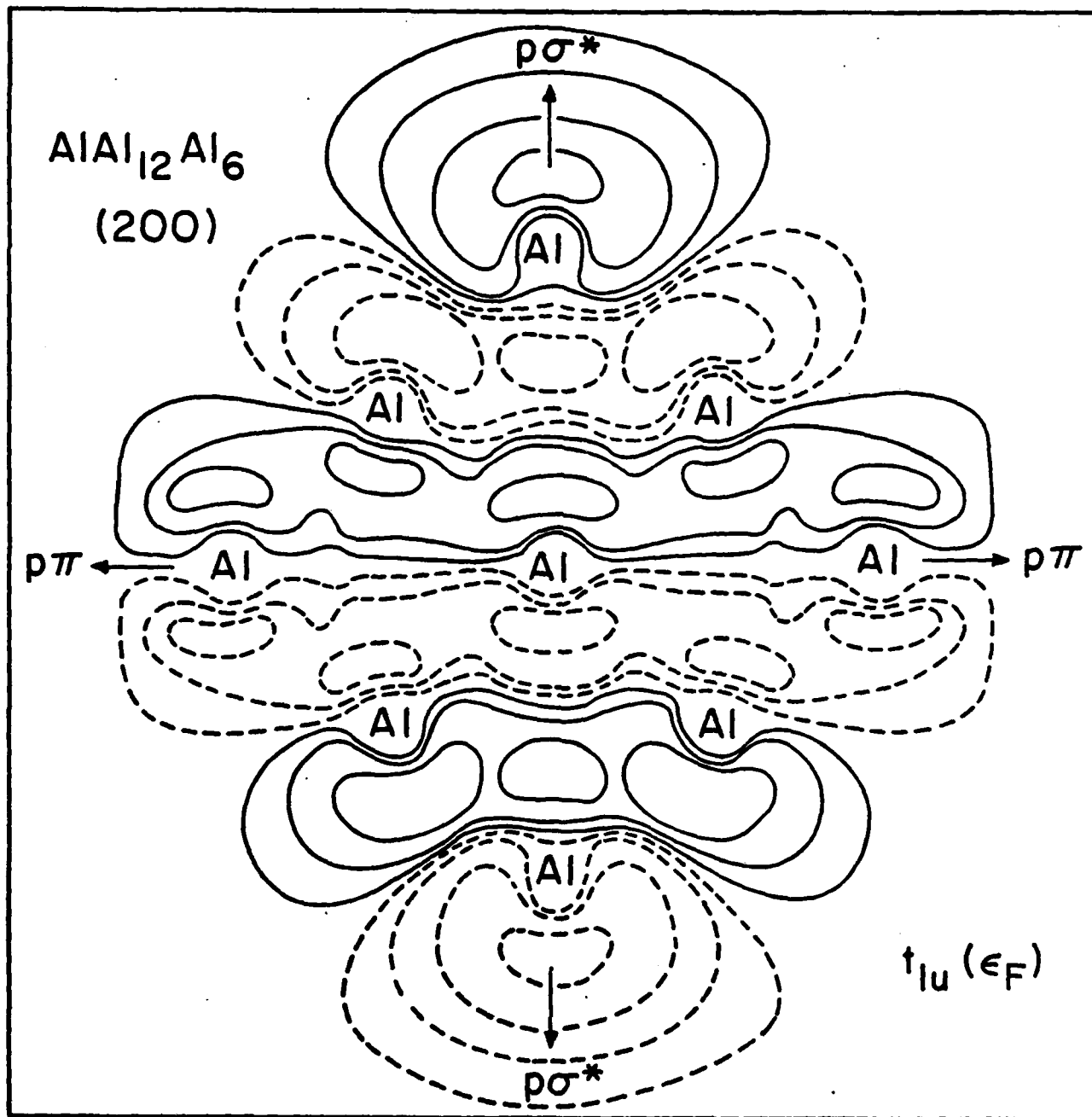


Figure 5

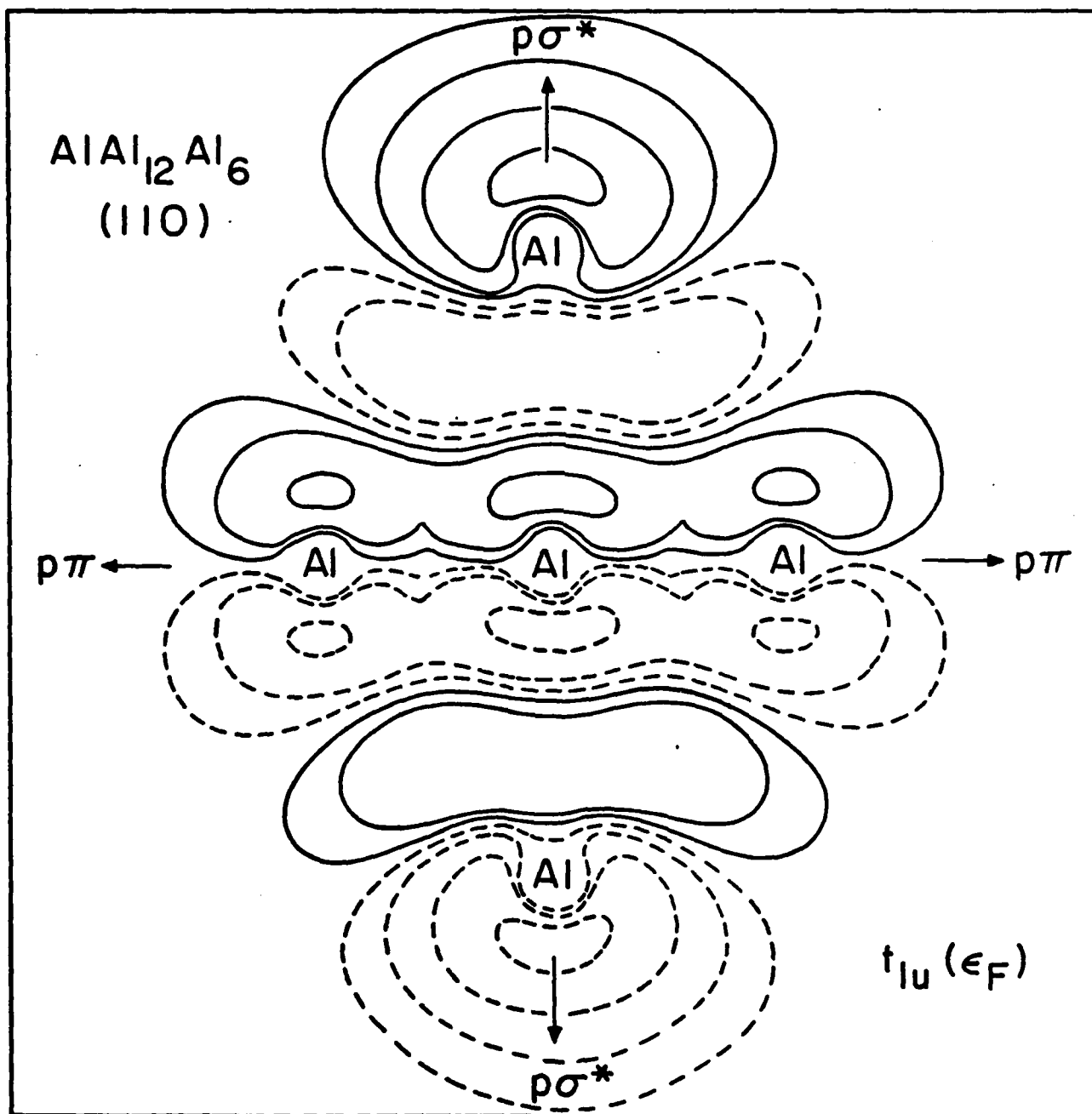


Figure 6

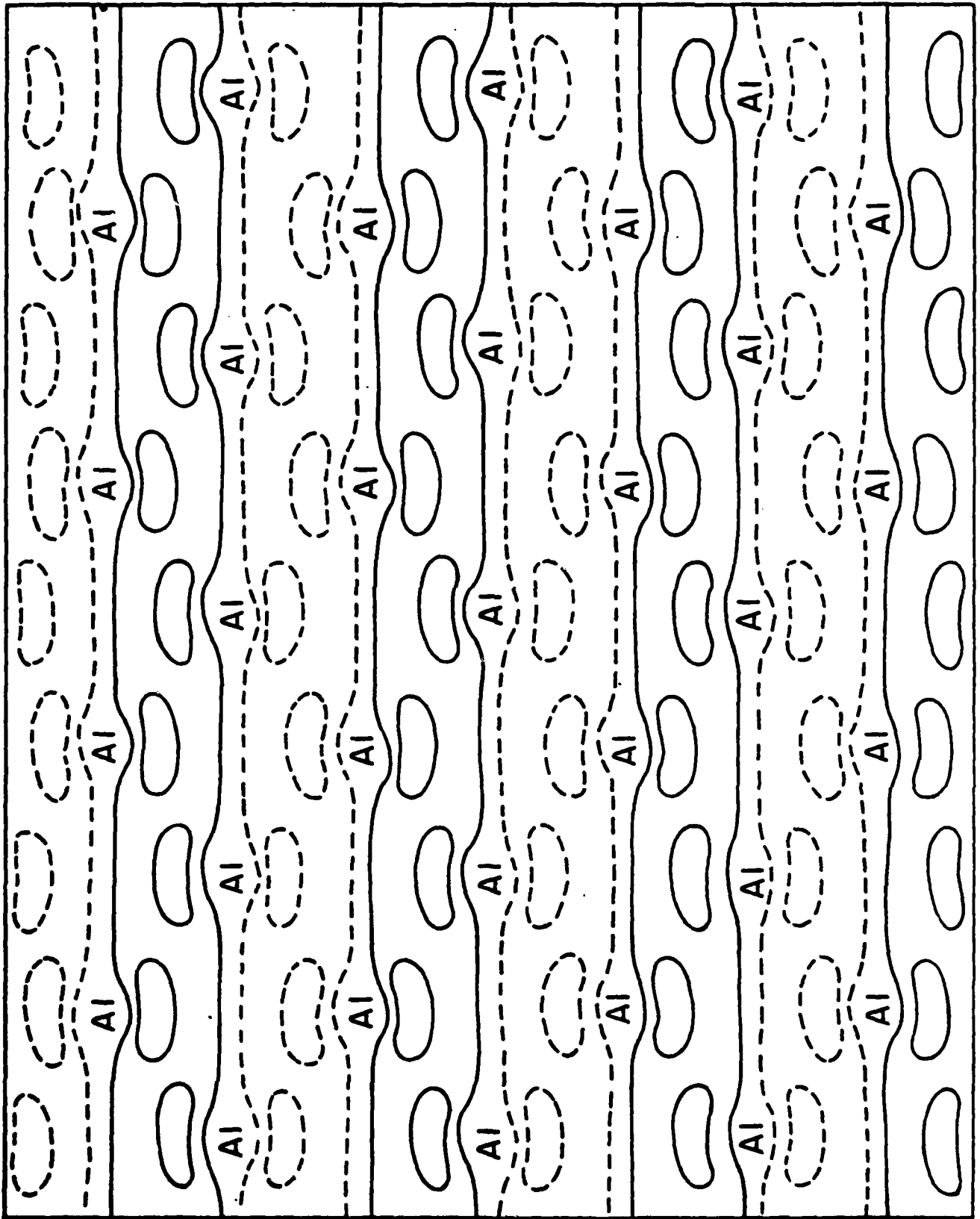


Figure 7

$\rho\pi$

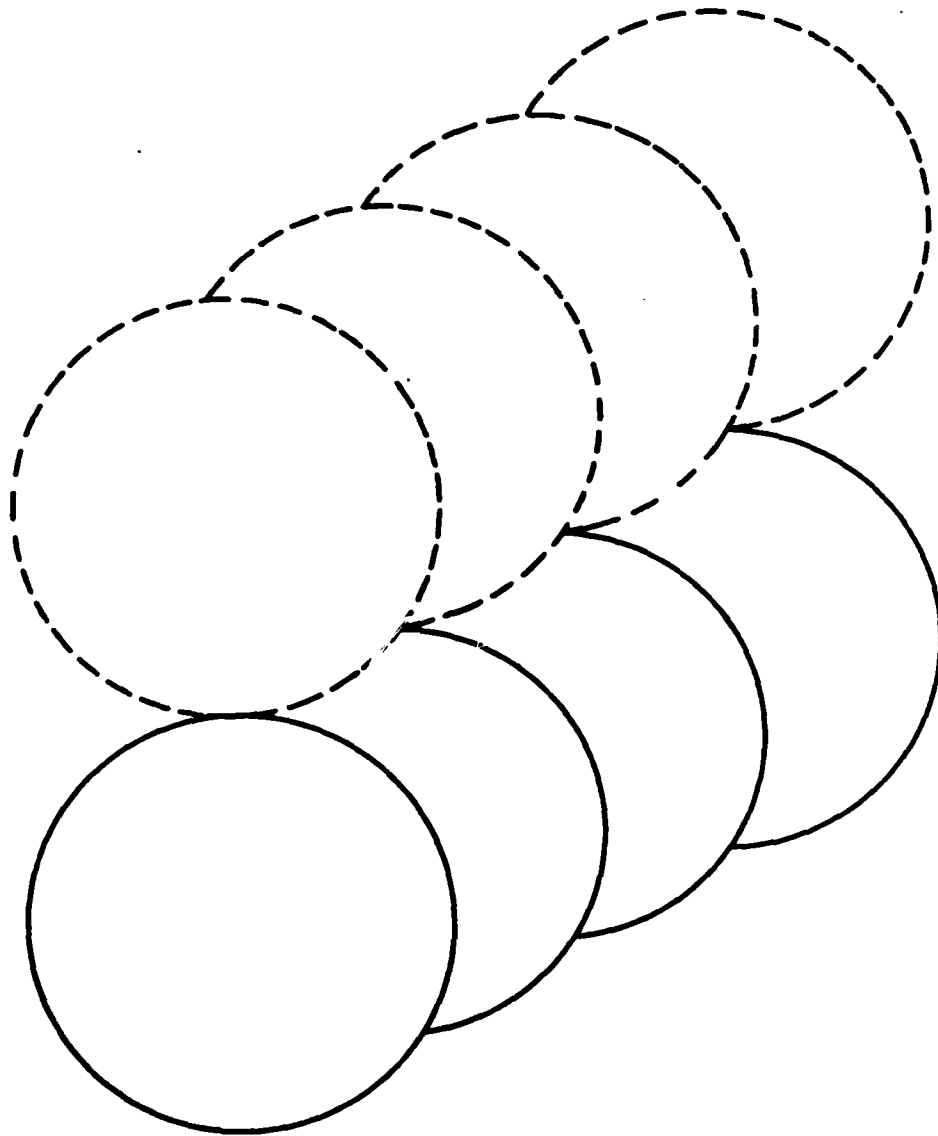


Figure 8

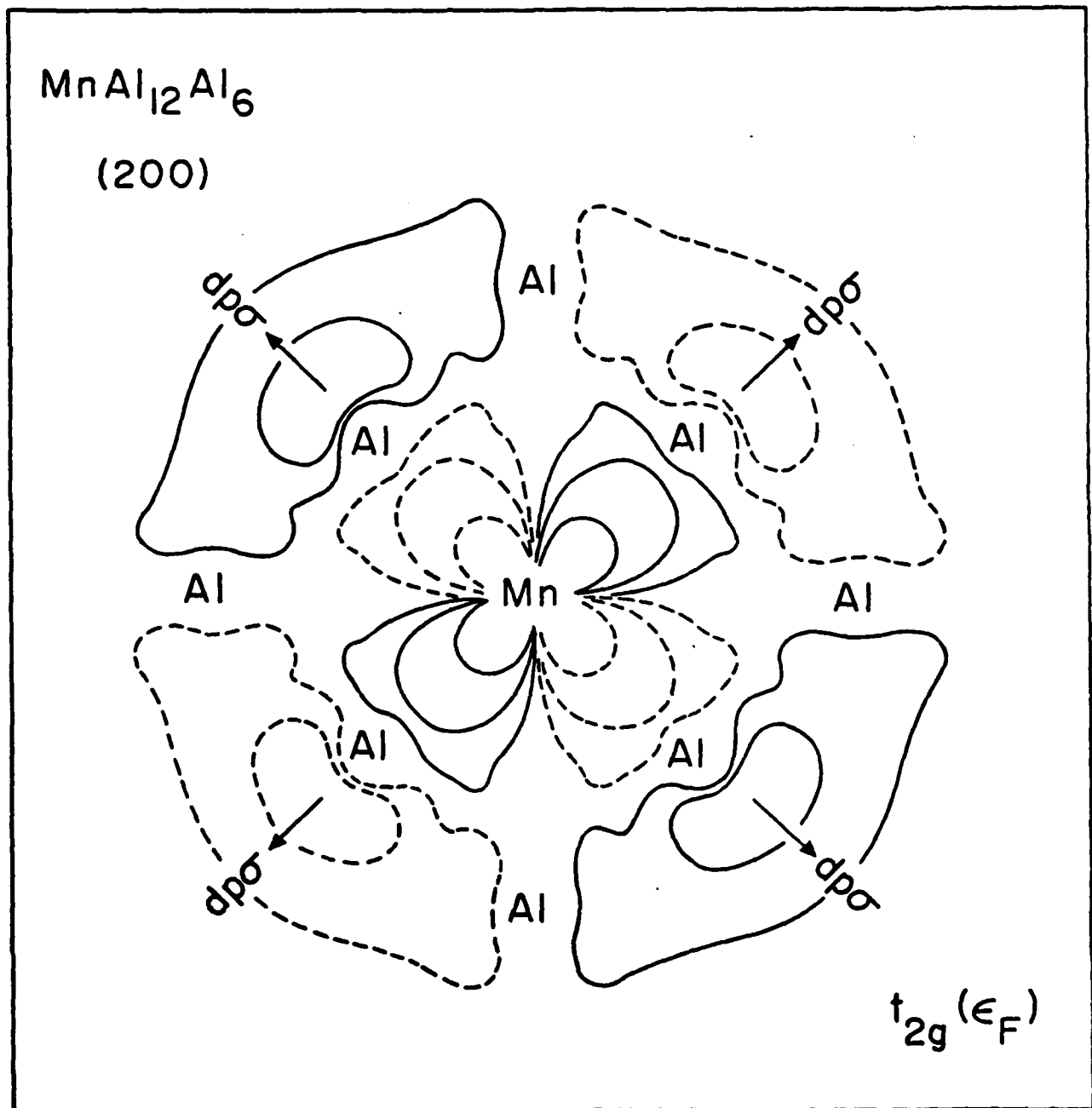


Figure 9

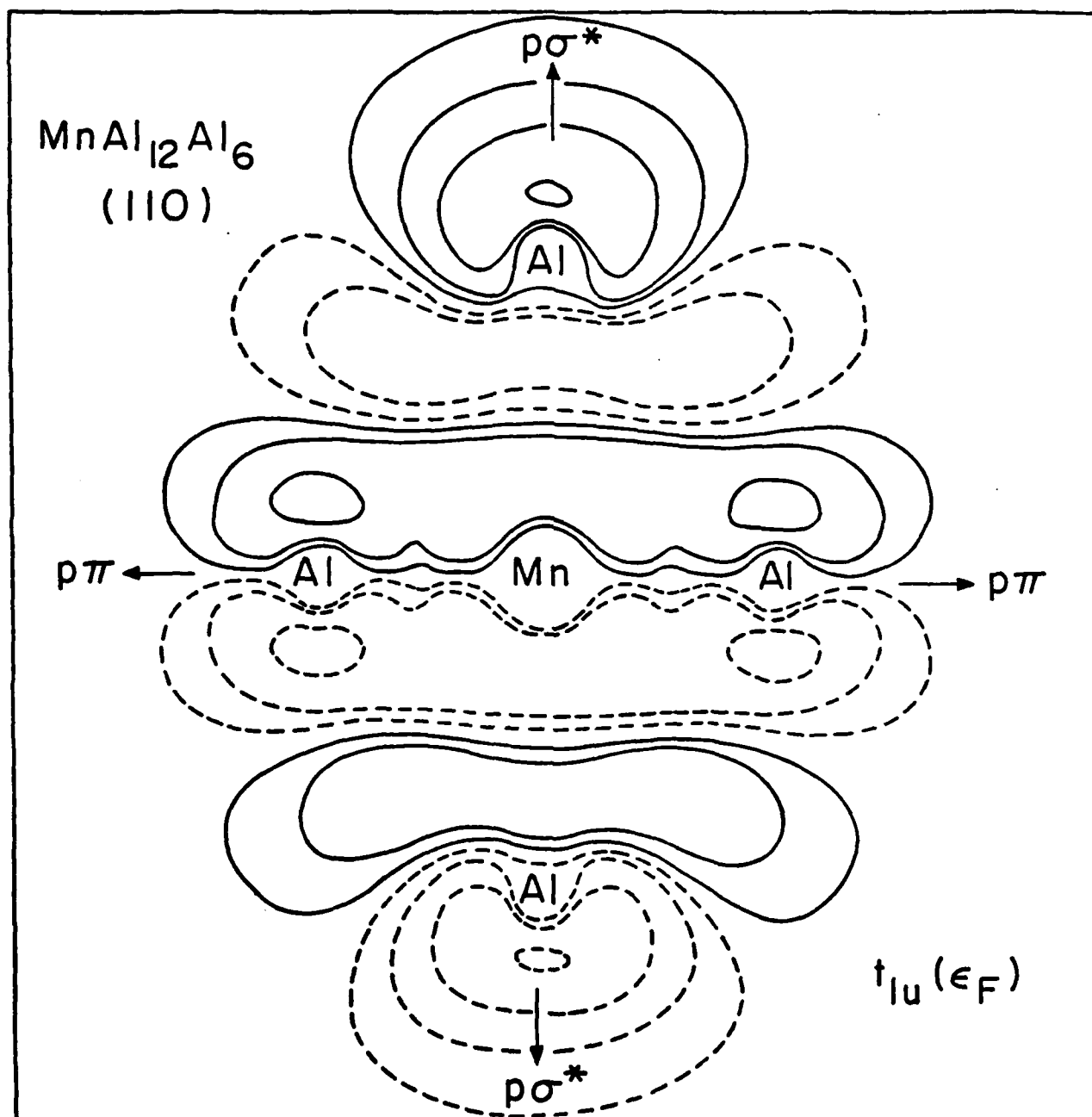


Figure 10

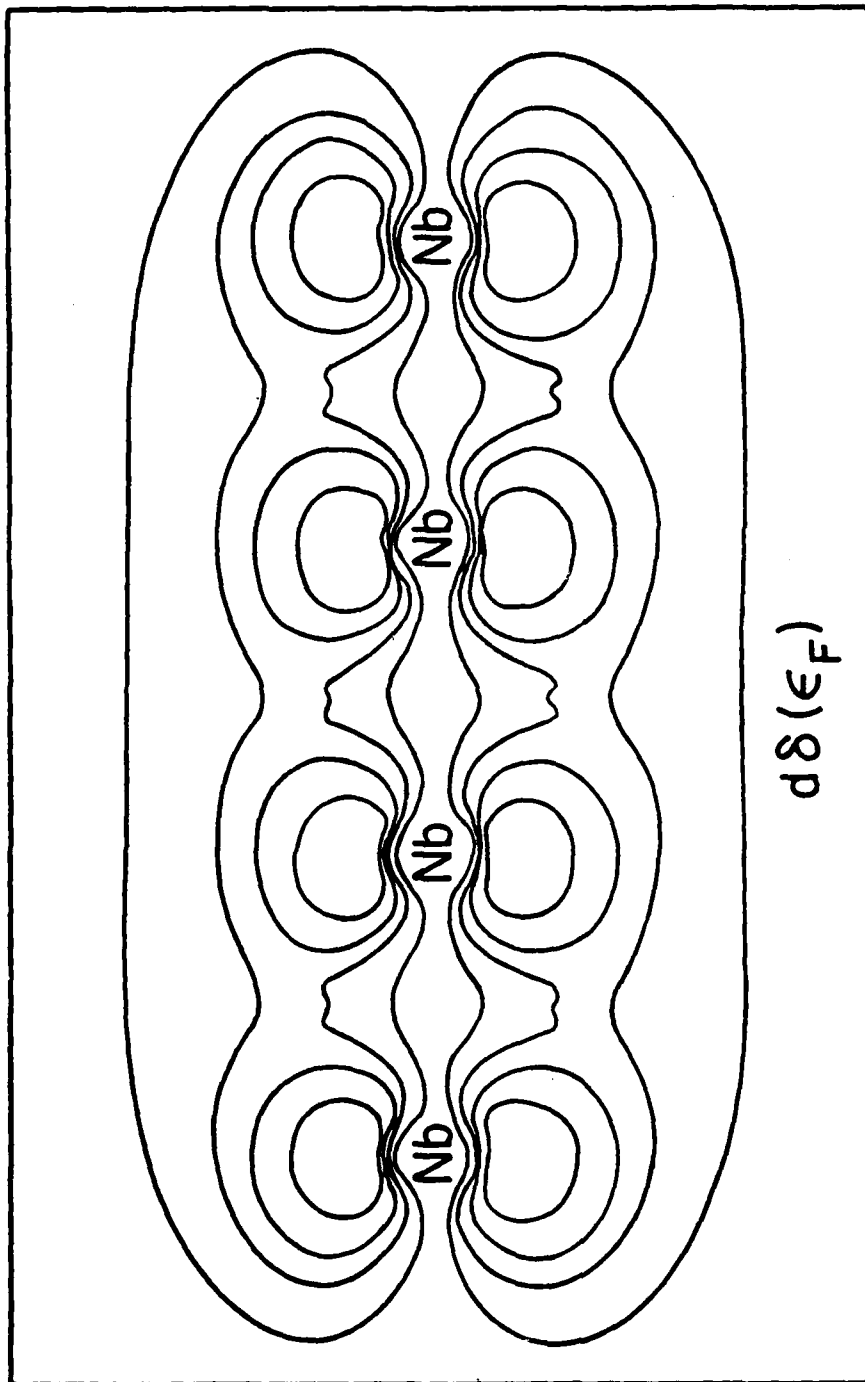


Figure 11

d δ

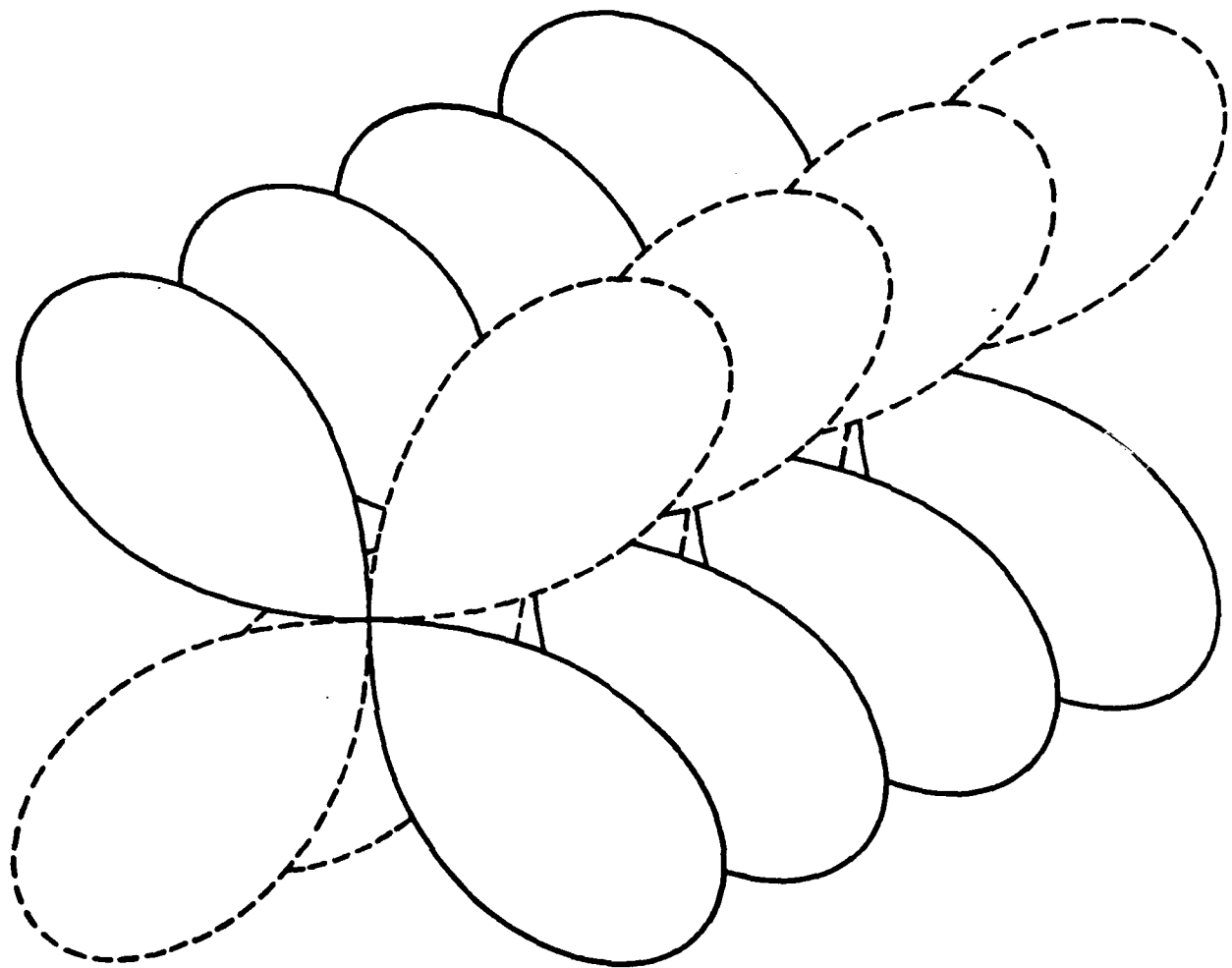


Figure 12

$d_{z^2}(a_1^*)$

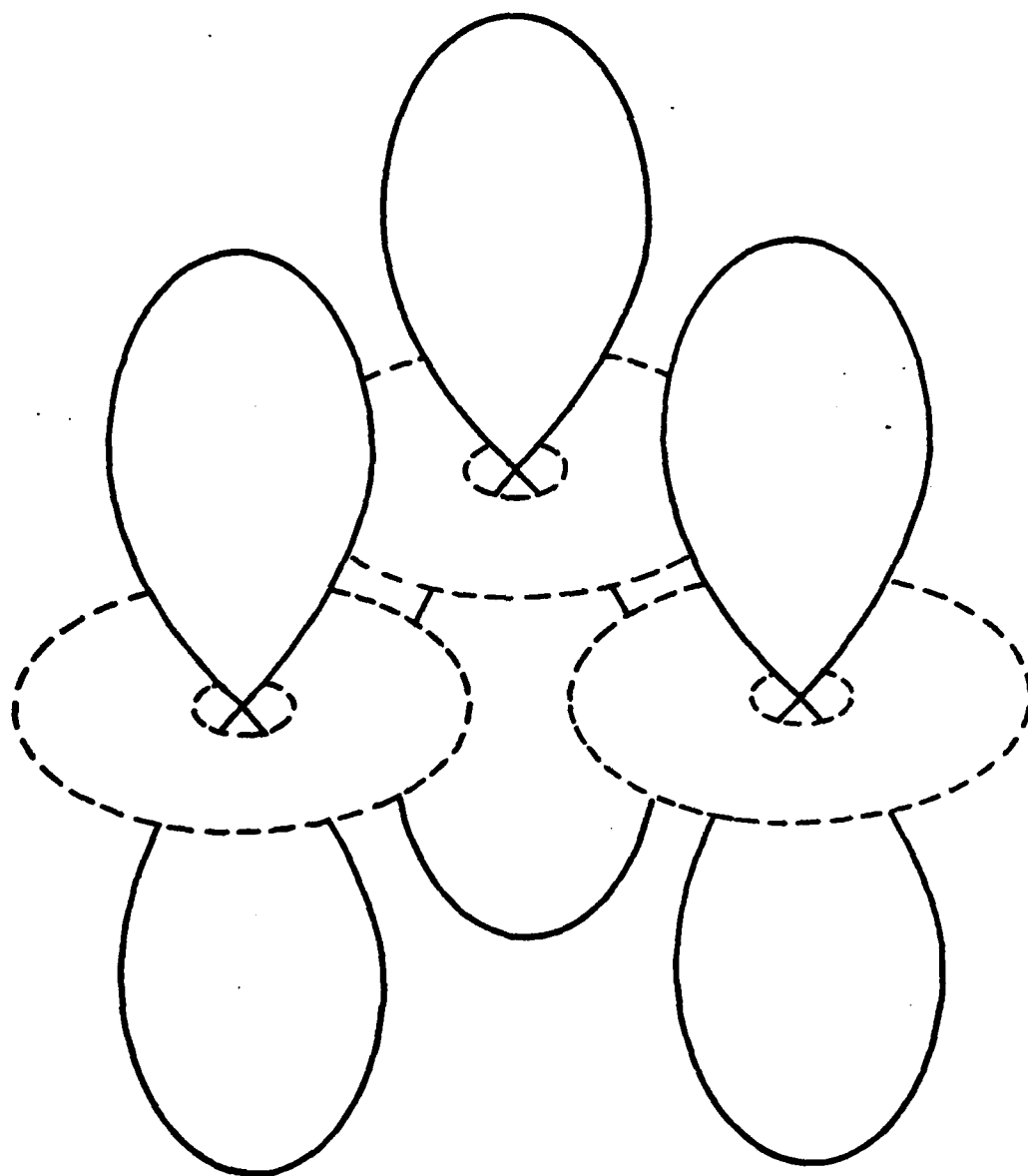


Figure 13

$S\sigma$

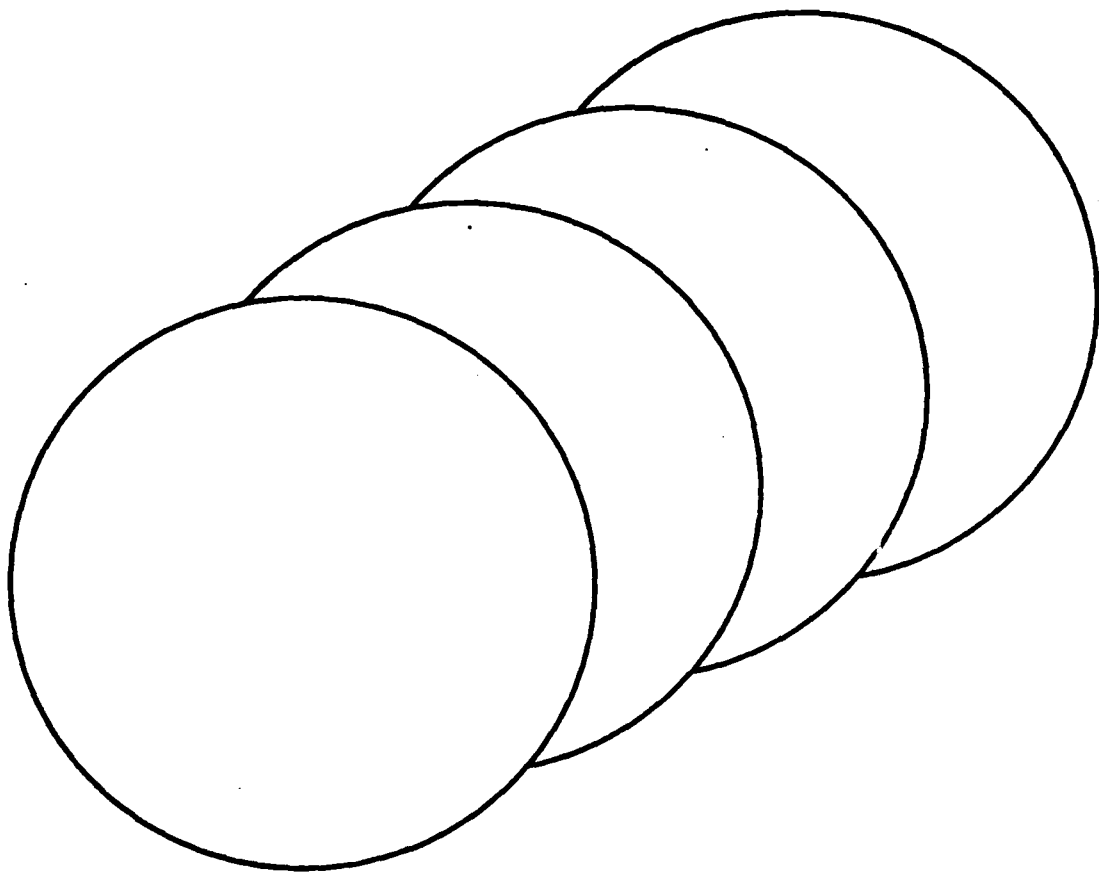


Figure 14